Ore Geology Reviews 72 (2016) 253–268

Contents lists available at ScienceDirect

Ore Geology Reviews

journal homepage: www.elsevier.com/locate/oregeorev

(Pb–Sb)-bearing sphalerite from the Čumavići polymetallic ore deposit, Podrinje Metallogenic District, East Bosnia and Herzegovina

Slobodan A. Radosavljević [a], Jovica N. Stojanović [a,*], Ana S. Radosavljević-Mihajlović [a], Nikola S. Vuković [b]

[a] Institute for Technology of Nuclear and Other Mineral Raw Materials, Applied Mineralogy Unit, Franchet d'Esperey 86, P.O. BOX 390, 11000 Belgrade, Serbia
[b] Laboratory for Scanning Electron Microscopy, Faculty of Mining and Geology, University of Belgrade, Djušina 7, 11000 Belgrade, Serbia

ARTICLE INFO

Article history:
Received 28 November 2014
Received in revised form 13 July 2015
Accepted 15 July 2015
Available online 17 July 2015

Keywords:
Sphalerite
Sulfosalts
Sb–Zn–Pb–Ag epithermal deposits
Čumavići
Srebrenica orefield

ABSTRACT

Čumavići is a medium– to low–temperature hydrothermal Sb–Zn–Pb–Ag polymetallic vein–type ore deposit in the Srebrenica orefield, part of the Podrinje Metallogenic District, Eastern Bosnia and Herzegovina. The ore deposit occurs in the form of simple and complex veins along faults and fractures, as well as stockworks and disseminations hosted within Neogene volcanic rocks (pyroclastics and andesite lavas of calc–alkaline affinity). The deposit comprises sulfides (sphalerite, galena, stibnite, pyrite, marcasite, chalcopyrite, arsenopyrite, gudmundite, safflorite, löllingite, gersdorffite and acanthite), sulfosalts (berthierite, geocronite, boulangerite, semseyite, plagionite, jamesonite, bournonite, twinnite, andorite, fizéliyte, Ag–bearing tetrahedrite, stephanite, polybasite, pyrargyrite and argyrodite), native gold and silver, tungstates (hübnerite), oxides, and gangue quartz, chalcedony, Mn–siderite, anglesite, smithsonite, fluorite, gypsum and ludlamite. Three generations of sphalerite are recognized in the Čumavići deposit, evolving from Fe–rich to Fe–poor. The most common are yellowish to colorless Fe–poor varieties. Electron Probe Microanalyses of sphalerite free of micro–inclusions of galena and Pb–Sb-sulfosalts revealed wide compositional variations in minor- and trace–element contents (e.g., Fe, Cd, Mn, Cu, Sn, As, and In). Of particular interest are the lead and antimony content of sphalerite, which vary from 0.10 to 3.08, and 0.02 to 1.62 wt.%, respectively. Lead– and Pb–Sb-rich zones are the most common in sphalerite, while individual Sb–bearing zones are rare. These zones have fan–like forms with circular to wave-like, micron–scale bands, filled with galena or Pb–Sb sulfosalts. In the Pb–Sb zones, the Sb/Pb atomic ratio ranges between 0.3 and 1.5, similar to ratios between geocronite and jamesonite, thus suggesting the presence of micro– to nano–scale inclusion of sulfosalts within the sphalerite. The mean composition of all sphalerite samples is $(Zn_{0.78–0.99},Fe_{<0.01–0.21},Cu_{0.00–0.02},Pb_{<0.01–0.01},Cd_{<0.01–0.01},Sb_{<0.01–0.01},Mn_{<0.01–0.01})_{\sum 0.97–1.03}S_{0.97–1.08}$ (Sn and As atomic proportions are <0.01 apfu). In all sphalerite samples, excellent negative correlations have been determined between Fe and Zn, and $\sum$(Fe + Sb) and Zn. The studied mineralization shares many mineralogical and geological characteristics in common to polymetallic Sn–Ag–Sb deposits in Bolivia and elsewhere.

1. Introduction

Sphalerite is an important host mineral for a wide range of minor– and trace–elements. The crystal structure of sphalerite is able to incorporate a large number of elements and a significant proportion of the Zn is commonly substituted by Fe, often by Cd, Cu and Mn, and to a minor extent by Mn, In, Sn, Sb, Ga, Ge, Tl, and Hg (e.g., Cook et al., 2009), either isomorphously or via one or more coupled substitutions. The chemical composition of sphalerite may be a useful indicator of conditions of formation, and varies significantly among different ore provinces. Sphalerite deposition takes place over wide temperature ranges (low–, medium– and high–temperature hydrothermal stages). The composition of sphalerite has commonly been used to decipher physico–chemical conditions of ore deposition, such as pressure, temperature and sulfur activity (e.g., Ramdohr, 1980; Sack and Ebel, 2006, and references therein).

Sphalerite deposited at higher temperatures commonly contains a large number of elements, which are later expelled from the structure as exsolution products (chalcopyrrhotite, pyrrhotite, chalcopyrite, talnakhite, and stannite). Iron–rich sphalerite is commonly also enriched in Mn, In, Cu, Co (high–temperature sphalerite), while those with low Fe content may contain Cd (up to 5 wt.%), Ge, Tl, Ga and Hg (low–temperature sphalerite) (Chvilyova et al., 1988).

The Podrinje Metallogenic District (PMD) belongs to the Serbo–Macedonian Metallogenic Province (SMMP) and incorporates several smaller orefields: Cer (Northwest Serbia), Boranja (West Serbia), and Srebrenica (East Bosnia & Herzegovina). The SMMP mainly hosts deposits of Tertiary age, although some Mesozoic and Late Paleozoic deposits are also present (Steiger et al., 1989; Karamata et al., 2000; Neubauer, 2002). Available radiometric ages indicate the onset of ultrapotassic volcanism around 30 Ma in the southern part of the

* Corresponding author.
E-mail address: j.stojanovic@itnms.ac.rs (J.N. Stojanović).

http://dx.doi.org/10.1016/j.oregeorev.2015.07.008
0169-1368/

province, along the NNE–SSW-trending Cer–Zvornik–Srebrenica line, where peripheral parts of the Srebrenica orefield (SOF) are located (Cvetković et al., 2004; Prelević et al., 2005).

The SOF includes numerous hydrothermal and greisen orebodies, hosted by Neogene subvolcanic rocks (mainly dacite, and lesser andesite), and less commonly, in Paleozoic slates and Neogene pyroclastic rocks. The orefield hosts two distinct types of mineralization: (i) cassiterite–bearing greisen–type mineralization related to quartz–tourmaline–muscovite facies of greisen; and (ii) hydrothermal veins with Pb–Zn–Fe sulfides as the principal ore minerals, and containing variable concentrations of Ag, Sn and Sb (Janković, 1990; Janković et al., 1992; Cvetković et al., 2004; Radosavljević et al., 2005). It should be emphasized that mineralization in the SOF shares many mineralogical similarities to those from the Andean Ag–Sn belt (Schneidere, 1987; Fontboté et al., 1990; Lehmann et al., 1990; Arce-Burgoa and Goldfarb, 2009), as well as from Freiberg, Erzgebirge, Germany (Seifert and Sandmann, 2006), the Lavrion deposit, Greece (Voudouris et al., 2008), and the Baia Mare Metallogenic District, East Carpathians, Romania (e.g., Kouzmanov et al., 2005). Moreover, mineralization at the San José Ag–Sn deposit, Oruro, Bolivia (Keutsch and de Brodtkorb, 2008), contains a comparable mineral assemblage (cassiterite, stannite, miargyrite, pyrargyrite, andorite and Bi–bearing andorite, jamesonite, boulangerite, ramdohrite pyrite, chalcopyrite, argentian tetrahedrite, galena and sphalerite) to that observed in the Čumavići deposit.

The Čumavići deposit, situated in the Northwest ore system of the SOF, is virtually unknown to an international scientific audience (Fig. 1). It was discovered during the 1970s as a Sb–Zn–Pb–Ag sulfide polymetallic deposit with the following main minerals: sulfides, Fe–Sb, Pb–Sb, Pb–Ag–Sb, Ag–Sb, Ag–Cu–Sb and Ag–Ge sulfosalts, native silver and gold, hübnerite, oxides of Sb, Mn and Pb, and gangue minerals. Rujevac is a similar Sb–Zn–Pb–As polymetallic deposit, located in the Boranja orefield, 20 km NNE from Čumavići (Janković et al., 1977; Borodaev, 1978; Moëlo et al., 1983; Radosavljević et al., 2012, 2014, Fig. 1).

The aims of the present study are to evaluate the geological, mineralogical and chemical characteristics of the Čumavići polymetallic deposit and to contribute to the knowledge of mineral associations, parageneses and the genesis of the medium– to low–temperature Pb–Zn–Ag–Sb polymetallic deposits of the SOF. Special emphasis is given to the optical, chemical and crystallographic characteristics of sphalerite. Identification of elevated Pb and Sb contents in sphalerite from the Čumavići and other Pb–Zn deposits within the SOF is of importance for environmental reasons, since these toxic elements can be easily released during mining and processing of zinc concentrates.

2. Geological setting and metallogeny of the Srebrenica orefield

The ore deposits of the SMMP, a portion of the Alpine metallogenic belt, lie within three main geotectonic units: the Vardar zone, the Serbo–Macedonian massif, and a small part of the Dinarides. This metallogenic province has been delimited mostly by reference to Paleogene–Neogene metallogeny, related predominantly to emplacement of granodiorite. The SMMP is located in the zone of tectonic–magmatic (re–)activation during the Cenozoic. Cenozoic tectonic activity and associated magmatism in Serbia is expressed by emplacement of two groups of igneous rocks: i) granitoids (Cer, Bukulja, etc.); and ii) multi–phase granodiorite volcanogenic–intrusive complexes (Podrinje, Kopaonik, Kratovo-Zletovo, etc.). The second group is genetically related to economically significant deposits of Pb–Zn, Sb, Cu, Mo, Au, and Fe (Petković, 1997). The PMD lies within the SMMP and includes several orefields:

(i) The Boranja orefield (BOF) was formed around the Boranja granitoid (West Serbia). Sporadic occurrences of granitoid–

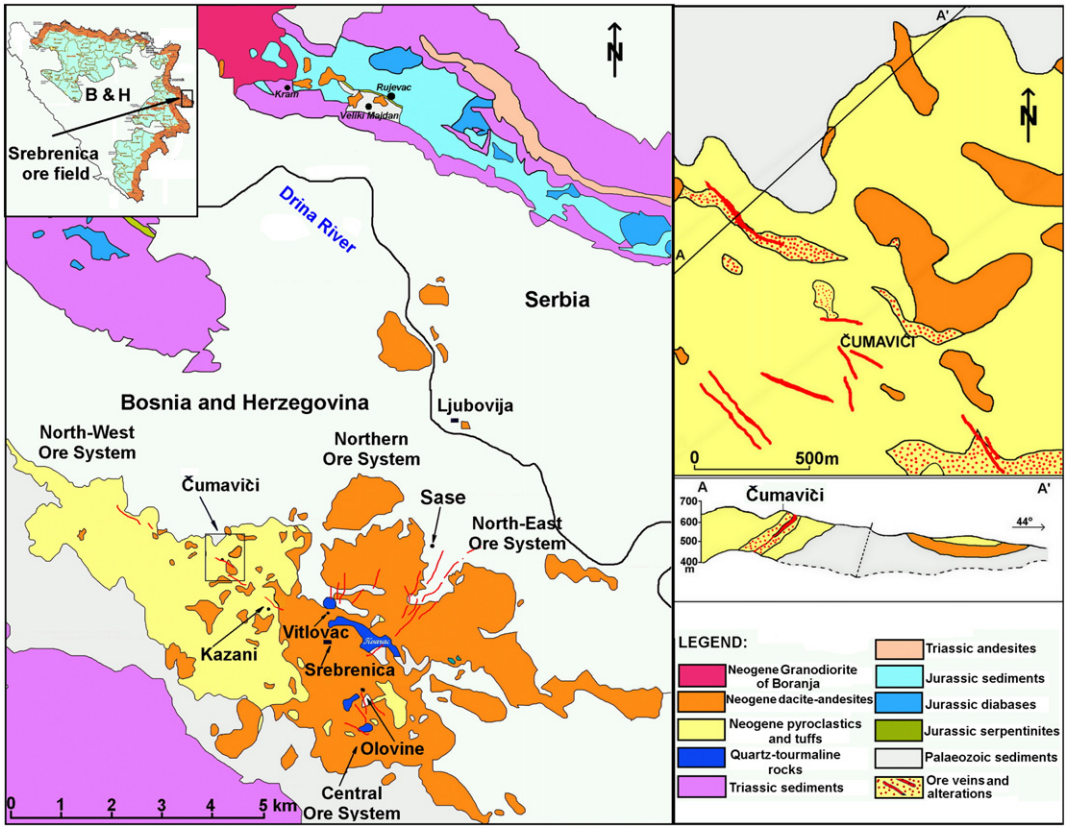

Fig. 1. Geological map of the SOF (Basic Geological Map of Serbia 1:100,000, Ljubovija sheet) and schematic geological plan of the Čumavići deposit across geological profile A–A′. Modified after Topalović (1984).

hosted greisen mineralization and a contact halo characterized by skarn deposits (Fe, Bi, Co), grade outwards through the Pb(Ag)-Zn zone, to the Sb–zone, in which the Veliki Majdan deposit is the most significant, but others (Zajača, Stolice, Brasina, etc.) are also known. The outermost zone includes the Rujevac and Ravnaja polymetallic Sb–Pb–Zn–As and fluorite–Pb–Zn deposits, respectively (Radosavljević et al., 2013).

(ii) The Cer orefield (Northwest Serbia) is developed within the Cer granitoid, and consists of small pegmatite bodies and occurrences of greisen mineralization (Sn, Bi and Nb–Ta).

(iii) The SOF (East Bosnia and Herzegovina).

The SOF, known since the Roman Empire, is characterized by high Pb(Ag)–Zn grades and by complex ore mineral assemblages. The SOF includes numerous hydrothermal ore veins and greisen orebodies, hosted mainly in Neogene calc–alkaline volcanics (mainly dacite, lesser andesite), and to a lesser extent, in Paleozoic slates and Miocene pyroclastic rocks (Ramović, 1963; Kubat, 1995). Two different types of mineralization constitute the SOF: (i) greisen–type mineralization, related to a quartz–tourmaline–muscovite rocks (S–type granitoid) with cassiterite (Zarić et al., 2000); and (ii) hydrothermal vein–type ores with Pb–Zn–Fe sulfides and variable amounts of Ag, Sn, Sb. Ramović (1963) and Radosavljević (1988) reviewed the main characteristics of Pb–Zn mineralization within the SOF.

Mineralization is related to ring–radial volcanic fractures. The hydrothermal vein–type ores are concentrated within four main systems of brecciated fractures (Fig. 1): (i) the Northeast ore system (the Sase mine); (ii) the Northwest ore system (the Kazani mine, Čumavići, Čumurnica, Mihajlovići, etc.); (iii) the Northern ore system (Vitlovac, Divljakinje, Čardaklije, Kvarac); and (iv) the Central ore system (Guber, Olovine, Vukosavljevići, etc.). Mineralization is genetically associated with a concealed (plutonic?) body of S–type granitoid composition emplaced some 5 km beneath the central part of the orefield (Petković and Romić, 1980; Janković et al., 1992; Vukašinović and Stefanović, 2003) (Fig. 1).

Greisen–style alteration and associated tin mineralization occurs particularly in the Kvarac area (Fig. 1). Greisens, composed of a quartz–tourmaline–muscovite assemblage with cassiterite, are developed along the contact between Neogene dacites and Paleozoic slates. Tourmaline is needle–shaped, zoned (central zones are light–green to colorless, and peripheral zones are dark–green), columnar to radiating aggregates ("tourmaline suns"). A multistage model can explain tourmaline growth. Mg–Fe rich hydrothermal fluids that produced the two tourmaline varieties (uvite and feruvite) represent the selective replacement of Paleozoic sediments and Neogene dacites (Radosavljević et al., 2011). In some greisen deposits such as some ore deposits of New Zealand (e.g., greisenized granite — Pirajno, 1992), as a corollary to such processes, the altered rocks in the lower zones of Sn-system are depleted in Sn. In the SOF, tin (as cassiterite) is concentrated in the upper levels of the greisen mineralization, whereas sulfides dominate at lower levels.

Lead–Zn sulfides, accompanied by marcasite, sulfosalts, Ag–minerals, Mn–siderite, and quartz are the dominant ore minerals of the SOF, and mainly occur in the central part of the orefield. In peripheral parts, low–temperature hydrothermal veins enriched in Sb, locally also in W and Hg, are present. The individual vein–type ores are characterized by variable thickness, length and complex morphology, within intensely brecciated portions of galena–sphalerite–marcasite ores. The most important ore veins are >2 km in length. The thickness of ore veins ranges from 0.5 m to over 5 m, sporadically up to 17 m. Over 100 hydrothermal vein–type ores have been discovery in the SOF, but only 20 of them have been exploited. The most significant vein–type ores are concentrated in the Northeast system (i.e., the Sase mine). Wall rocks are strongly hydrothermally altered (silicified, kaolinized, sericitized, chloritized); the alteration pattern displays a lateral zoning with increasing distance from the ore veins (Dangić, 1978).

2.1. Geology of the Čumavići deposit

Carboniferous sediments and metamorphic rocks, mostly phyllites, slates, sandstones, metasandstones are the oldest rocks in the Northwest ore system of the SOF. Neogene volcanics, part of the Srebrenica volcanic complex, strike NW–SE, and cover a surface area of about 80 km^2. Volcanic rocks (e.g., lavas and pyroclastics) are the main host rocks for Sb–Zn–Pb–Ag mineralization. Their thickness varies (up to 300 m), depending on morphology of current relief and paleomorphology of the schist–sandstone basement (Topalović, 1984).

The Northwest ore system characterizes numerous polymetallic orebodies connected to NW–trending fault–fissure structures, running parallel to the trend of the volcanic complex, and to the deep lineament located on the SW border of the volcanic complex. This lineament facilitated magma ascent and late hydrothermal activity in the Northwest ore system. Host rock lithology played also a significant role in the localization of orebodies and precipitation of sulfide mineralization.

The Čumavići deposit is an economically important system of Sb–Pb–Zn–Ag vein ores, a few tens of meters in length, filling faults and fissures of the volcanic complex. The orebodies dip to SW at an angle of 30–80°. The ore occurs in three types: 1) massive to brecciated or crustiform–banded vein-type mineralization; 2) stockworks in hydrothermally–altered volcanic rocks; and 3) disseminations.

Vein–type mineralization was discovered by drilling and has been named the main or "Čumavići" ore vein. This orebody is up to 3.8 m in thickness and fills the NW–trending fault zone. It grades outwards into weakly mineralized hydrothermally altered zones (Fig. 2a). Smaller (up to 1 m–thick) veins, parallel to subparallel to the main ore vein, are highly enriched in Sb, Pb, Zn, Ag, and Au. Ore textures are brecciated, massive and crustiform–colloform banded (Fig. 2b, c).

The stockwork mineralization is characterized by a network of thin (cm–dm in length and mm–cm–thick) veins, unevenly distributed in volcanic rocks.

The disseminated style of mineralization occurs as nest-like fine–grained impregnations of ore and accompanying minerals. Irregular, thin (mm– to cm–scale) veinlets occur sporadically within the hydrothermally altered rock mass.

3. Materials and analytical methods

Ore samples were collected from trenches and drill holes during the period 1973 to 1984 in order to obtain mineralogical data for the Northwest ore system (Kazani, Čumavići, Kutlići, Mihajlovići and Ćumurnica; Radosavljević, 1988). Two hundred and fifteen polished–sections of sulfide ore were prepared for reflected–light microscopy and Electron Probe Micro–analyses (EPMA) by following standard preparation and polishing steps (Picot and Johan, 1982).

EPMA was carried out at the Faculty of Mining and Geology, the University of Belgrade, using a JEOL JSM–6610LV scanning electron microscope (SEM) equipped with an INCA energy–dispersive X–ray analysis unit (EDS). An acceleration voltage of 20 kV was used. The analyzed samples were coated with carbon (15 nm thick layer, density 2.25 g/cm^3). For quantitative analyses the following synthetic standards were used: $CuFeS_2$ (Fe Kα), ZnS (Zn Kα), Mn (Mn Kα), $CuFeS_2$ (Cu Kα), Gadolinium Gallium Garnet (Ga Kα), Ge (Ge Lα), InAs (As Kα, In Lα), InSb (Sb Lα), SnO_2 (Sn Lα), Ag_2Te (Ag Lα), CdS (Cd Lα, S Kα), PbS (Pb Mα), and Bi (Bi Mα). EDX detection limit of 2σ ~0.3 wt.%. Part of the EPMA work was carried out on a Cambridge Scientific Instruments, Microscan M-9, equipped with two WDS analytical systems (Institute "Jozef Stefan", Ljubljana, Slovenia), using the following natural standards: PbS (Pb Mα), (Zn, Fe)S (Zn Kα, Fe Kα, S Kα), Sb_2S_3 (Sb Lα), Bi_2S_3 (Bi Mα), $CuFeS_2$ (Cu Kα) and synthetic standards: CdS (Cd Lα, S Kα), Ag (Ag Lα), InAs (As Kα, In Lα), Sn (Sn Lα). The results were corrected, for absorption and atomic number effects (ZAF corrections). WDS detection limit for all elements was ~0.01 wt.%. Chemical formulae were calculated according to Anthony et al. (1990).

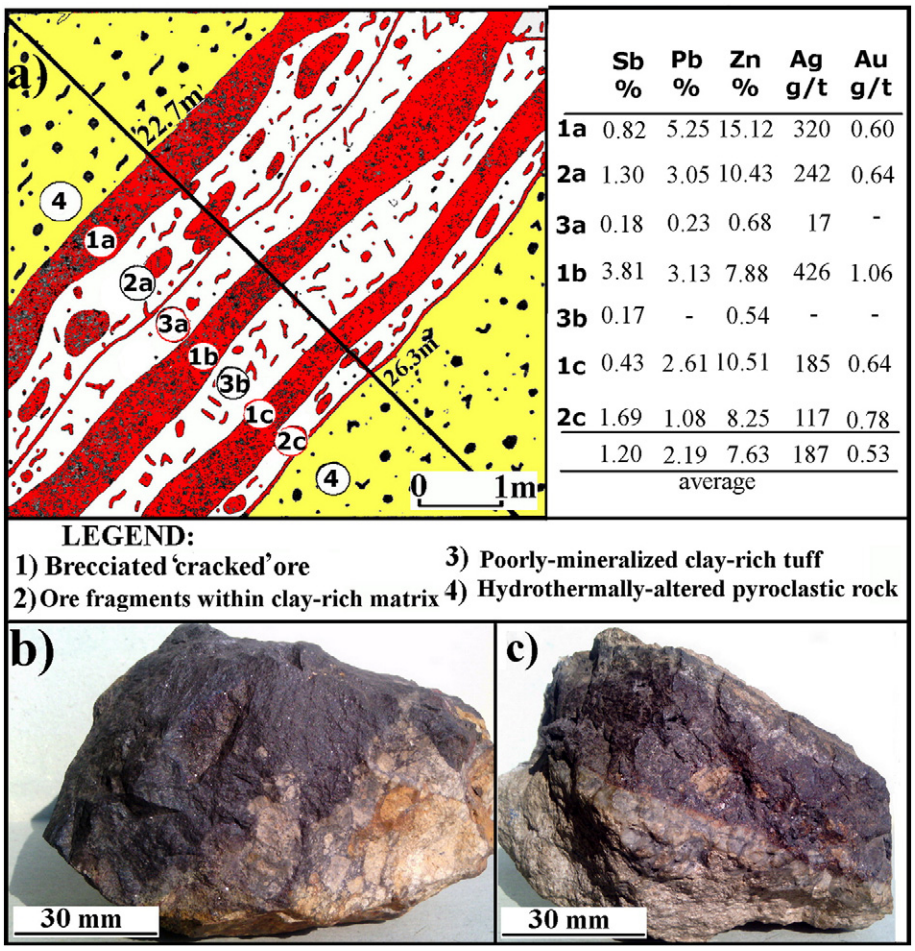

	Sb %	Pb %	Zn %	Ag g/t	Au g/t
1a	0.82	5.25	15.12	320	0.60
2a	1.30	3.05	10.43	242	0.64
3a	0.18	0.23	0.68	17	-
1b	3.81	3.13	7.88	426	1.06
3b	0.17	-	0.54	-	-
1c	0.43	2.61	10.51	185	0.64
2c	1.69	1.08	8.25	117	0.78
	1.20	2.19	7.63	187	0.53
	average				

Fig. 2. a) Geological profile of the "Čumavići" ore vein (after Topalović, 1984); b) hand specimen of massive ore within brecciated pyroclastic host rock; c) hand specimen demonstrating banded sphalerite–rich veinlet (up to 3 cm in width) embedded in hydrothermally–altered pyroclastic rock.

Mass spectrometric analysis (MSA) of pure sphalerite grains was conducted using a JEOL, model 01 MB mass spectrometer (analytical range 1000–0.01 ppm). Iron content from sphalerite determined by Atomic Absorption Spectroscopy (AAS–Perkin Elmer AA–300) was used as a standard for MSA.

In addition, contents of Sb, Zn, Pb, and As were also determined by AAS, while Au and Ag were obtained by the cupellation method for all ore samples.

The X–ray powder diffraction (XRPD) method was used to determine the unit–cell parameters of sphalerite and galena. The XRPD patterns were obtained on a Philips PW–1710 automated diffractometer using a Cu tube operated at 40 kV and 30 mA. The instrument was equipped with a diffracted beam curved graphite monochromator and a Xe–filled proportional counter. The diffraction data were collected in 2θ Bragg angle range from 4 to 80°, counting for 0.5 s (qualitative identification) and 5 s (calculation of the unit–cell parameters) at every 0.02° step. The divergence and receiving slits were fixed at 1 and 0.1, respectively. All XRPD measurements were performed at room temperature in a stationary sample holder. The LSUCRIPC (least square unit–cell refinement) program was used for the refinement of the unit–cell parameters from the powder data (Garvey, 1986).

4. Bulk ore geochemistry

Orebodies of the Čumavići polymetallic deposit are characterized by complex intergrowths of ore minerals, ranging from Sb–ores enriched in Pb and Zn to Pb–Zn ores enriched in Sb. Compositional changes occur even within short distances (dm–m in length, and one to several dm thick), indicating abrupt changes in fluid composition (Fig. 2a). The orebodies are also characterized by a wide spectrum of metal associations. The main ore metals are Sb, Pb, Zn, and Ag, while Au, W, and As occur locally.

The average chemical composition of the "Čumavići" ore vein was obtained from 20 analyses of representative trench samples taken along vein strike. The thickness of the vein ranges from 0.1 to 5.2 m [average 1.14 m; coefficient of variation Cv = (standard deviation/mean value) × 100 = 125%]. Antimony content of the mineralization ranges from 0.08 to 26.80 wt.% (average 3.45 wt.%; Cv 143%). Lead and zinc contents are also very variable and range from 0.04 to 7.02 (average 1.25 wt.%; Cv 141%), and from 0.25 to 12.62 wt.% (average 3.29 wt.%; Cv 90%), respectively. Ag content ranges from 17 to 1165 g/t (average 117 g/t; Cv 123%). Au content varies from 0.4 to 23 g/t. The As content ranges from 0.1 to 1.5 wt.%. The average WO_3 content is 0.12 wt.%. Contents of minor- and trace-elements are as follows (g/t): 10–200 Sn, 3–20 Ga, 0–5 Mo, 3–30 Ni, <1–7 Co, 3–80 Cr, <1–55 La, 10–1700 Ba, <1–400 Sr. Copper, In, Ge, and Tl were not analyzed.

During detailed geological mapping of the Čumavići area at 1:2500 scale, the following chemical composition of a representative ore sample was determined: 0.65–5.60 wt.% Cu, 0.05–1.31 wt.% Sb and 0.34–6.30 wt.% Pb. Silver contents range from 22 to 200 g/t (Kubat, 1995).

5. Paragenetic relationships

Deposition of minerals within ore systems of the SOF occurred in several successive stages within a single mineralization event. The

contact–pneumatolytic stage characteristic for greisens (quartz–tourmaline rocks) with strong mineralization of Ti, Sn and Rare Earth Elements (REE) occurs in the Northern ore system, and to a lesser extent, in the Central and Northeast ore system. According to the mineral associations, the hydrothermal stage can be divided in several substages: high-, hypogene, medium and low–temperature. The hydrothermal stage occurs to the fullest extent and characterizes high abundance and the number of deposited minerals. On the basis of deposited minerals, it can be concluded that the hydrothermal solutions have common magmatic origin (Rakić, 1962). According to the δS^{34} isotopic analyses of stibnite from Čumavići, sulfur in sulfides is of magmatic origin (Kubat, 1995). Values ranging from +3.7 to −4.97‰, (average −0.37‰) are similar to those of meteorites (Thode et al., 1961). Substages and paragenetic sequences of ore and gangue minerals within the Northwest ore system of the SOF are shown in Table 1.

The following mineralization substages (paragenetic sequences) were determined within the Čumavići deposit: a) medium–temperature hydrothermal (sphalerite–galena–marcasite–Mn–siderite); b) low–temperature hydrothermal (b1 quartz–sphalerite–galena-sulfosalts, b2 quartz–sphalerite–berthierite–hübnerite, and b3 chalcopyrite–Ge–Ag–Au-sulfosalts); and c) supergene.

The sphalerite–galena–marcasite–Mn–siderite paragenetic sequence is the most widespread in the SOF. It is geologically the most significant and contributes most of the Pb–Zn mineralization in the SOF. Sphalerite I and galena occur in a form of veins, veinlets, lenses, and nests, and are accompanied by Mn–siderite and marcasite. Ore minerals are banded, occasionally with wavy textures composed of individual sub–mm– to cm–scale layers. Vein walls are dominated by Mn–siderite and marcasite. Coarse, crystalline Fe–rich sphalerite occurs in the outer parts of the veins, while galena, sulfosalts, and quartz crystals fill the central parts of the veins.

The quartz–sphalerite–galena-sulfosalt paragenetic sequence was deposited during the low–temperature hydrothermal substage. It marks either the end of the previous mineral substage, usually located in the central parts of the veins, or it is partly synchronous with it. Sphalerite II, associated with galena, is characterized by colloform bands. Lead–Sb(Fe,Cu) sulfosalts fill open spaces between idioblastic quartz grains, or form reaction rims around corroded aggregates of galena.

The quartz–sphalerite–berthierite–hübnerite paragenetic sequence is characteristic for the Northwest (Čumavići), and the Northern (Vitlovac, Kiselica) ore systems (Fig. 1). It is associated with the low–temperature hydrothermal substage composed of a large number of minerals: Fe–poor sphalerite (III generation), berthierite, stibnite, hübnerite, arsenopyrite, safflorite, gudmundite, and quartz (mostly chalcedony). Ag–minerals are less abundant, and restricted to small crystals of andorite.

The chalcopyrite–Ge–Ag–Au-sulfosalt paragenetic sequence occurs only in the Northwest ore system. It is unique throughout the SMMP on the territory of Eastern B&H, Serbia and Former Yugoslav Republic of Macedonia (FYRM). Andorite, argentian tetrahedrite, stephanite, polybasite, pyrargyrite, and argyrodite are the Ag–bearing minerals identified. Lead–Sb sulfosalts are represented by geocronite, boulangerite, semseyite, plagionite, jamesonite, bournonite, twinnite; quartz and chalcedony are accessory minerals.

All paragenetic sequences of the Čumavići deposit tend to overlap with one another, forming complex mineral associations both within the main ore vein and its apophyses or mineralized zones. An important feature for the Čumavići deposit and throughout the orefield is the occurrence of a diverse range of Sb–, Pb–, Ag–, Fe–, Cu– and Ge–bearing sulfosalts (Rakić et al., 2003; Radosavljević et al., 2013).

6. Ore mineralogy

Ore minerals consist of sulfides (sphalerite, galena, stibnite, pyrite, marcasite, chalcopyrite, arsenopyrite, gudmundite, safflorite, löllingite, gersdorffite, acanthite), sulfosalts (berthierite, geocronite, boulangerite, semseyite, plagionite, jamesonite, bournonite, twinnite, andorite, fizéliyte, Ag–rich tetrahedrite, stephanite, polybasite, pyrargyrite, argyrodite), native gold and silver, tungstates (hübnerite), oxides (valentinite, senarmontite, kermesite, Mn–oxides, W–oxides), and gangue minerals (quartz, chalcedony, Mn–siderite, rhodochrosite, anglesite, smithsonite, fluorite, gypsum, ludlamite). These are described below taking their paragenetic relations into consideration.

6.1. Sulfides

Sphalerite, determined throughout SOF, occurs in four generations and is more abundant than galena. According to optical features it belongs to both Fe–rich (marmatite), as well as Fe–poor variety (cleophane) (Radosavljević, 1988). The first and oldest generation is very rich in Fe and is widespread in quartz–tourmaline greisens of the Northern (Vitlovac), Central (Olovine), and Northeast (Sase mine) ore systems (Fig. 1). The second, also Fe-rich generation, is widespread in the Northern (Vitlovac, Kiselica) and the Northeast (Sase) ore systems, while in the Northwest ore system it occurs only sporadically (Kazani, Čumavići) (Fig. 1). The third generation is Fe-poor, and is widespread in the Northwest ore system (Čumavići, Čumurnica, Kutlići). The fourth generation is almost Fe–free, and volumetrically insignificant for the SOF (Radosavljević et al., 1990).

In the Čumavići deposit, sphalerite occurs in three generations (Table 1). The first (sphalerite I) is Fe–rich, free of inclusions of Fe–, Cu–, Sn–sulfide minerals and associated with galena and carbonate (Mn–siderite) matrix. Along its rim, sphalerite is brecciated and cemented by galena, jamesonite and bournonite (Fig. 3a). Its grain margins are characterized by intense internal reflections (Fig. 3b). Sphalerite II (Fig. 4a, b) is also Fe–rich and occurs in spongy–colloform

Table 1
Substages and paragenetic sequences of ore and gangue minerals within the Northwest ore system of the SOF (according to Radosavljević, 1988, updated by this study).

Substages	Paragenetic sequences	Deposits
High-temperature hydrothermal	Quartz I–pyrrhotite I–magnetite–rutile–arsenopyrite I	Kazani***, Mihajlovići*
	Quartz II–sphalerite I–pyrrhotite II–chalcopyrite I–petrukite–tetrahedrite I–galena I–native silver I–falkmanite	
Hypogene	Marcasite I–pyrite I–hematite	Kazani**
Medium-temperature hydrothermal	Mn–siderite–marcasite II–sphalerite II–chalcopyrite II–stannite–galena II–± sternbergite–jamesonite I–semseyite I–plagionite–boulangerite I (plumosite)–± argentite–quartz II	Northwest ore system***–**
Low-temperature hydrothermal	Quartz III–arsenopyrite II–sphalerite III–galena III–native silver II–Ag-bearing tetrahedrite–chalcopyrite II–bournonite–semseyite II–polybasite–geocronite–plagionite–twinnite–boulangerite II	Northwest ore system***–*
	Quartz IV–± hübnerite–± berthierite–± gudmundite–stibnite–pyrite II–± gersdorffite–safflorite–löllingite–chalcedony	
	Rhodochrosite–marcasite III–sphalerite IV–galena IV–chalcopyrite III–Ag(Au)–bearing tetrahedrite–native gold–argyrodite–stephanite–pyrargyrite–andorite–fizélyite–acanthite–jamesonite II–boulangerite III–fluorite–gypsum–ludlamite	Čumavići***
Supergene	Kermesite–valentinite–senarmontite–Mn-oxides–± W-oxides–anglesite–cerussite–smithsonite–limonite–goethite	Northwest ore system***–*

Note: *** Main; **Weak; * Trace.

textures, also forming complex intergrowths with galena and Sb–Pb-sulfosalts (Fig. 3c–e). Moreover, rare Sn–Cu sphalerite belongs to this generation (Fig. 8f). This variety is quite abundant in the Vitlovac locality–Northern ore system (Radosavljević, et al., 2011; Zarić, et al., 2000). Sphalerite III, the most abundant sphalerite generation, is Fe–poor. It occurs in coarse crystalline aggregates commonly brecciated and cemented by quartz (Figs. 3f and 4c). It is intensively overgrown and penetrated by needle– to lath–like crystals of berthierite (Fig. 3 g, h). Intergrowths of Sb–, Pb– and/or Sb–Pb–sulfides/sulfosalts also occur in distinct growth zones within sphalerite (Figs. 3i–k and 4d–e).

Galena is the second most abundant ore mineral in the SOF after sphalerite. Three generations are recognized in the Čumavići polymetallic deposit. The first generation is synchronous with Fe–rich sphalerite and is associated with arsenopyrite in a carbonate matrix (Mn–siderite). The younger generations (galena II and III) are associated with colloform sphalerite, sulfosalts, and Ag–minerals (Fig. 3a, e). It usually replaces sphalerite when forming complex aggregates composed of sphalerite relics and Pb–Sb sulfosalts. Spherical sphalerite bands frequently occur in porous galena (Figs. 3f and 4a–c). Similar oscillatory zoning in galena from the Herja deposit, Baia Mare district, Romania, was recently published by George et al. (2015). Like other sulfides, galena can be compositionally zoned at the grain–scale. Given the non–metamorphosed character of this young deposit (~10 Ma), zoning must have developed during initial crystallization. Oscillatory zoning in galena can be interpreted either as an intrinsic or an extrinsic phenomenon, i.e., relating to crystal growth within a closed, local system, or involving chemical fluctuations in the ore–forming fluid. Zoning possibly relates to crystallization in a locally closed system within the larger, open hydrothermal system (George et al., 2015).

Besides sphalerite and galena, Fe–sulfides are also very abundant in the SOF. Marcasite is dominant and makes most of the ore mass, together with Mn–siderite. Pyrite is less frequent and mostly occurs in

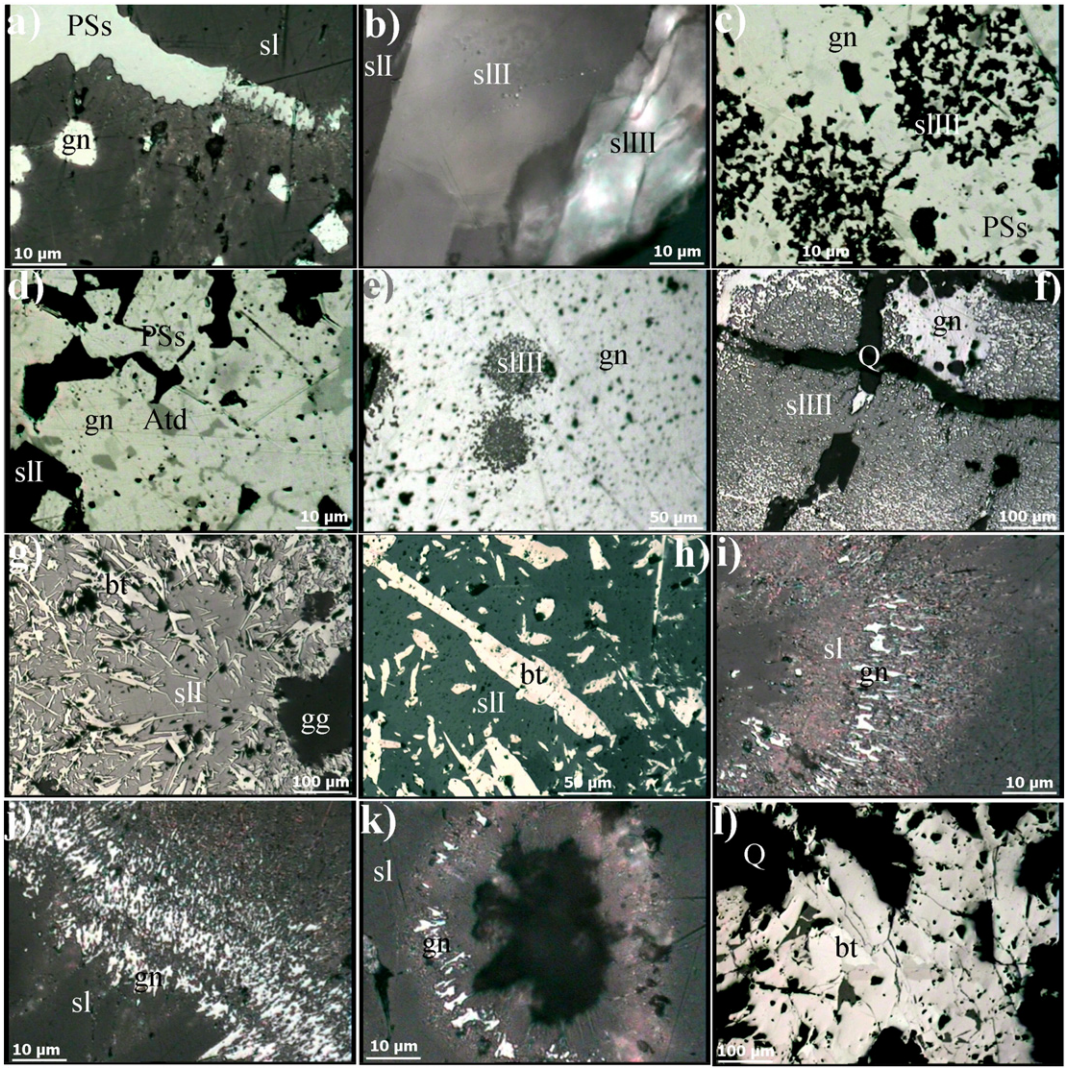

Fig. 3. Reflected light photomicrographs showing textural characteristics of sphalerite from the Čumavići deposit: a) all three generations of cataclastic sphalerite cemented with Pb–Sb sulfosalts (light gray) and galena (white) (oil, //N); b) parallel bands of all three generations of sphalerite (color change is a function of Fe content) (oil, ×N); c) a spherical, spongy aggregate of sphalerite III grains (black) accompanied with Pb–Sb sulfosalts and galena (white to light gray) (oil, //N); d) a mixed aggregate composed of galena (creamy white), Ag–bearing tetrahedrite (dark gray), Pb–Sb sulfosalts (light gray), and sphalerite I (black) (oil, //N); e) a porous aggregate of galena with spherical–spongy grains of recrystallized sphalerite III (gray) (air, //N); f) cataclastic mixed aggregate of sphalerite III and galena cemented with quartz (black) (air, //N); g) a sphalerite I aggregate including prismatic and needle–like crystals of berthierite embedded in carbonate matrix (air, //N); h) Sphalerite I including prismatic crystals of berthierite (air, //N); i) needle–like to dotted micron to submicron inclusions of Pb–Sb sulfosalts and galena in sphalerite (II and III) with pale red internal reflections (oil, //N); j) multilayer wavy needle–like to dotted micron to sub–μm inclusions of Pb–Sb sulfosalts and galena (white) in sphalerite (II and III) with pale red internal reflections (oil, //N); k) annular, needle–like and dotted micron to submicron inclusion of Pb–Sb sulfosalts and galena in sphalerite (II and III) with pale red internal reflections (oil, //N); l) Irregular monomineral aggregate composed of prismatic crystals of berthierite (strong bireflectance from light creamy white to light brown with reddish tinge) embedded in quartz matrix (air, //N). Abbreviations: gn — galena, sl — sphalerite (sII, sIII, sIIII — sphalerite of I, II and III generation), PSs — Pb–Sb sulfosalts, Atd — Ag-bearing tetrahedrite, bt — berthierite, gg — gangue minerals, Q — quartz.

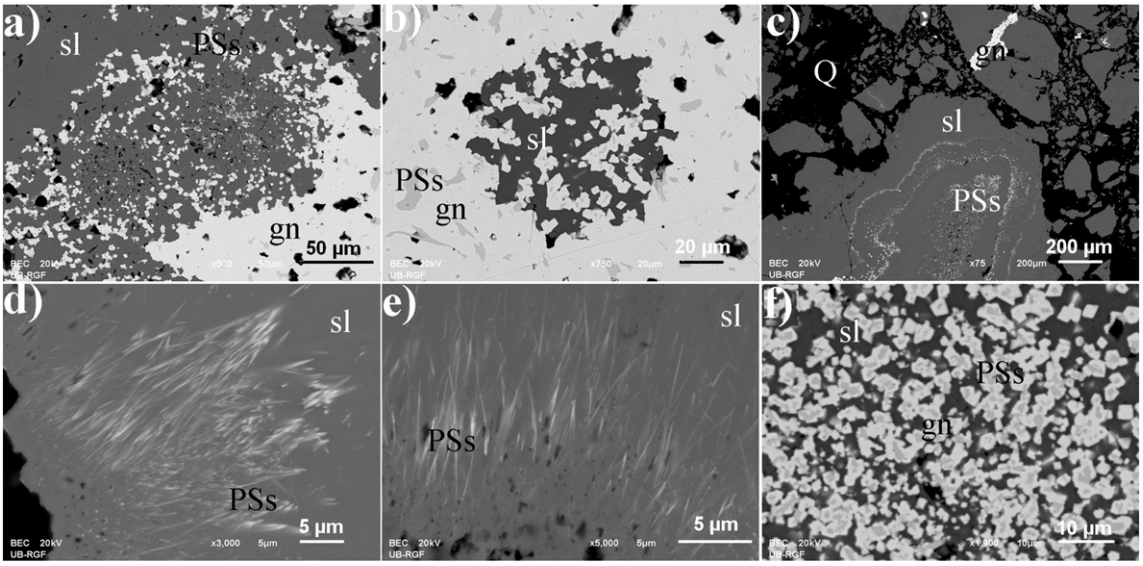

Fig. 4. SEM-BEI photomicrographs of textural characteristics of sphalerite III from the Čumavići deposit: a) an aggregate composed of spongy sphalerite (gray), galena and Pb–Sb sulfosalts (light gray); b) a spherical–spongy sphalerite (dark gray) accompanied by Pb–Sb sulfosalts (shades of gray) and galena (white); c) a cataclastic aggregate of sphalerite (gray) with wavy–colloform inclusions of Pb–Sb sulfosalts and galena (white), cemented by quartz (black); d) fibrous micron to submicron inclusions of Pb–Sb sulfosalts (white) in sphalerite; e) fibrous micron to submicron inclusions of Pb–Sb sulfosalts (white) in sphalerite; f) an assemblage of micron-size sphalerite (dark gray matrix) → galena (white) → Pb–Sb sulfosalts (light gray). Abbreviations: gn — galena, sl — sphalerite, PSs — Pb–Sb-sulfosalts.

high–temperature parts of the ore veins at the SOF (Olovine, Vitlovac, Čardaklije, etc.). EPMA yielded an almost ideal stoichiometric chemical composition for marcasite, while pyrite is characterized by elevated As content (up to 2.08 wt.%).

Only moderate amounts of chalcopyrite are present. The mineral is mostly associated with sulfosalts (e.g., bournonite and boulangerite), as well as with gold are rare Ag–Ge-minerals. EPMA yielded an ideal stoichiometric chemical composition for chalcopyrite with some analyses displaying elevated Ga content (up to 0.70 wt.%). Individual Ga-minerals have not been determined.

Stibnite occurs throughout the SOF, notably in the Northern and Northwest ore system. In some ore veins within the Čumavići polymetallic deposit, it is the main Sb–mineral, forming massive and fibrous aggregates cemented by quartz. The amount of stibnite in the ore is, however, significantly lower than that of berthierite. Quantitative EDS analyses yielded stoichiometric chemical compositions, without presence of any other element. Geodes are characterized by idiomorphic radial stibnite crystals (Zebec, 1982).

Gudmundite occurs in regular small crystals embedded in quartz matrix. It is a rare phase present in the sphalerite–berthierite mineral association and is accompanied by marcasite, safflorite, arsenopyrite and pyrargyrite.

Acanthite is associated with chalcopyrite, Ag–Ge and Pb–Sb sulfosalts. It is often intergrown with chalcopyrite, which indicates that this mineral was probably exsolved from pre–existing polybasite. EPMA yielded following chemical composition: $(Ag_{1.80},Cu_{0.11},Fe_{0.02},Pb_{0.02})_{\sum 1.95}S_{1.05}$.

Safflorite, determined only microscopically, is very rare and occurs with marcasite, arsenopyrite, and sulfosalts in a quartz matrix.

Table 2
Average EPMA of sulfosalts from the quartz–sphalerite–galena–sulfosalts and chalcopyrite–Ge–Ag–Au-sulfosalts mineral assemblages (in wt.%).

Mineral	(n)	S	Mn	Fe	Cu	Zn	As	Ag	Cd	Sb	Pb	Au	Total
Berthierite	(4)	29.85	0.51	12.72	–	–	–	–	–	56.78	–	–	99.86
(apfu)		3.99	0.04	0.98						2.00			7
Geocronite	(1)	18.13	–	–	–	3.44	–	–	–	18.10	59.99	–	99.66
(apfu)		23.02				2.14				6.05	11.79		43
Boulangerite	(2)	18.86	–	–	–	–	–	–	–	25.41	55.95	–	100.22
(apfu)		11.03								3.91	5.06		20
Semseyite	(12)	19.32	–	–	–	0.51	–	–	–	27.56	52.34	–	99.73
(apfu)		20.99	–	–		0.27	–			7.89	8.80		38
Bournonite	(4)	19.79	–	–	13.11	–	–	–	–	24.38	42.56	–	99.84
(apfu)		3.01			1.01					0.98	1.00		6
Jamesonite	(13)	21.54	–	2.61	–	–	–	–	–	35.24	40.43	–	99.82
(apfu)		13.94	–	0.97						6.01	4.05		25
Plagionite	(2)	20.94	–	–	–	–	–	–	–	38.24	40.54	–	99.84
(apfu)		16.85								8.10	5.05		30
Pyrargyrite	(5)	18.14	–	0.87	2.35	–	–	54.70	0.85	22.78	–	–	99.69
(apfu)		3.00		0.08	0.20			2.69	0.04	0.99			7
Andorite	(4)	22.18	–	0.42	–	–	–	11.71	–	41.84	23.44	–	99.59
(apfu)		6.02		0.07				0.94		2.99	0.98		11
Ag(Au)-bearing tetrahedrite	(2)	21.47	–	4.98	13.52	0.96	–	32.34	–	25.25	–	1.12	99.64
(apfu)		12.95		1.73	4.12	0.28		5.80		4.01			29
Ag(Fe)-bearing tetrahedrite	(4)	23.50	–	6.27	25.82	–	–	16.61	–	27.55	–	–	99.75
(apfu)		13.03		2.00	7.22			2.74		4.02			29
Ag(Zn)-bearing tetrahedrite	(3)	23.88	–	1.32	29.33	6.11	–	11.08	–	28.21	–	–	99.93
(apfu)		13.03		0.41	8.07	1.63		1.80		4.05			29

Note: (n) number of analyses; – below detection limits (< ~0.3 wt.%); EPMA — EDS-analytical system; (apfu) atoms per formula unit.

Table 3
Average EPMA* of sphalerite and sulfosalts from the Čumavići deposit (in wt.%).

Mineral	(n)	S	Mn	Fe	Cu	Zn	As	Ag	Cd	Sn	In	Sb	Pb	Bi	Total
Sphalerite I	(4)	33.50	0.69	8.48	–	56.82	n.a.	–	0.28	0.07	0.03	n.a.	n.a.	n.a.	99.87
(apfu)		1.004	0.012	0.146		0.835			0.002	0.001					2
Sphalerite II	(4)	33.55	0.55	6.54	0.33	58.27	n.a.	–	0.35	0.07	0.01	n.a.	n.a.	n.a.	99.67
(apfu)		1.009	0.010	0.113	0.005	0.860			0.003	0.001					2
Sphalerite III	(2)	33.27	0.01	1.31	–	64.56	n.a.	–	0.95	–	0.01	n.a.	n.a.	n.a.	100.11
(apfu)		1.009		0.023		0.960			0.008						2
Bournonite	(8)	19.40	–	0.03	12.86	–	–	–	n.a.	n.a.	n.a.	23.91	43.65	–	99.85
(apfu)		2.99			1.00							0.97	1.04		6
Boulangerite	(3)	18.05	–	0.01	0.01	–	–	0.05	n.a.	n.a.	n.a.	25.83	55.85	0.06	99.80
(apfu)		10.77						0.01				4.06	5.16		20
Jamesonite	(1)	21.72	–	2.53	–	–	–	0.16	n.a.	n.a.	n.a.	35.62	40.07	–	100.10
(apfu)		13.99		0.94				0.03				6.04	4.00		25
Twinnite	(2)	21.54	–	–	–	–	4.55	0.01	n.a.	n.a.	n.a.	33.87	40.49	–	100.46
(apfu)		3.90					0.35					1.61	1.13		7
Polybasite	(1)	15.16	–	0.04	2.66	0.08	–	69.91	n.a.	n.a.	n.a.	10.11	–	1.67	99.63
(apfu)		10.92		0.02	0.97	0.03		14.97				1.92		0.18	29
Stephanite	(2)	15.54	–	0.04	0.98	0.06	1.50	65.92	n.a.	n.a.	n.a.	15.78	–	0.12	99.94
(apfu)		3.84		0.01	0.12	0.01	0.16	4.84				1.03			10
Ag(Bi)-bearing tetrahedrite	(2)	22.71	–	5.54	23.38	1.27	0.28	19.56	n.a.	n.a.	n.a.	26.28	–	0.59	99.61
(apfu)		12.85		1.80	6.67	0.35	0.07	3.29				3.92		0.05	29
Andorite	(12)	22.37	–	0.59	0.09	0.01	–	11.90	n.a.	n.a.	n.a.	41.60	23.17	0.11	99.84
(apfu)		6.02		0.09	0.01			0.95				2.95	0.97		11
Fizélyte	(1)	20.93	–	1.49	0.04	–	–	8.04	n.a.	n.a.	n.a.	34.82	34.45	–	99.77
(apfu)		47.60		1.95	0.05			5.43				20.85	12.12		88

Note: (n) number of analyses; – below detection limits (< ~0.01 wt.%); n.a. not analyzed for; EPMA* — WDS-analytical system; (apfu) atoms per formula unit.

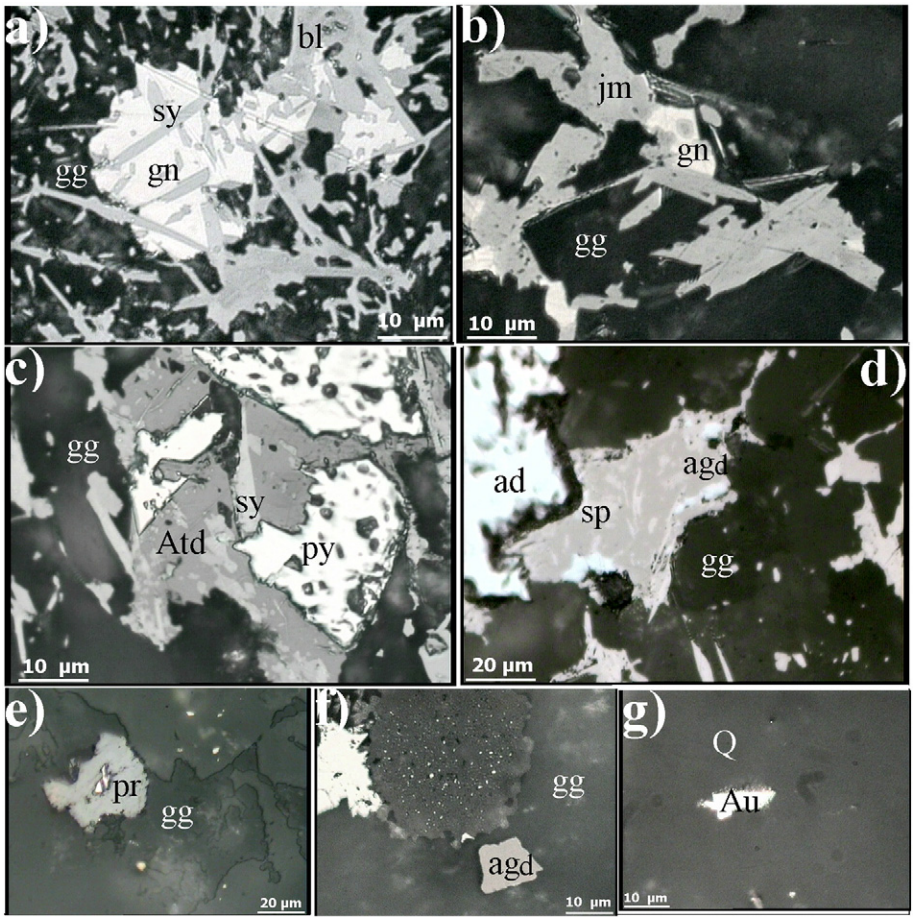

Fig. 5. Reflected light photomicrographs of textural characteristics of sulfosalts from the Čumavići deposit: a) galena (white) and quartz–carbonate matrix intersected by needle–like crystals of semseyite (light gray) and boulangerite (dark gray) (oil, //N); b) Jamesonite prismatic crystals and galena (white) in quartz matrix (black) (oil, //N); c) Ag–bearing tetrahedrite (dark gray) and younger semseyite (light gray), as cement of pyrite crystals (white) (oil, //N); d) an aggregate of argyrodite (dark pink) intergrown with stephanite (light pink) and andorite (light gray) (air, //N); e) pyrargyrite (gray) in carbonate matrix (air, //N); f) a trapezoidal cross–section of argyrodite (gray) embedded in carbonate matrix (oil, //N); g) native gold (light) in a quartz matrix (black) (oil, //N). Abbreviations: gn — galena, py — pyrite, sy — semseyite, Atd — Ag-bearing tetrahedrite, bl — boulangerite, jm — jamesonite, agd — argyrodite, sp — stephanite, ad — andorite, pr — pyrargyrite, gg — gangue minerals, Q — quartz.

Table 4
EPMA of argyrodite (1–12) from the Čumavići deposit (in wt.%).

Number of analysis	S	Fe	Cu	Zn	Ge	Ag	Cd	In	Au	Total
1	17.16	0.32	0.43	–	6.45	75.50	–	–	–	99.86
2	17.06	0.34	0.72	–	6.56	73.21	–	–	1.93	99.82
3	17.18	–	1.23	–	6.28	75.35	–	–	–	100.04
4	16.98	0.38	1.66	0.72	5.94	72.06	1.46	0.71	–	99.91
5	17.24	0.36	1.66	–	6.46	74.19	–	–	–	99.91
6	17.21	–	1.73	–	5.88	71.50	1.80	1.80	–	99.92
7	16.97	0.34	2.09	0.52	6.32	70.03	2.63	1.26	–	100.16
8	17.45	–	2.35	0.73	6.26	72.96	–	–	–	99.75
9	17.19	0.33	2.57	–	5.75	71.52	1.78	0.84	–	99.98
10	17.12	0.34	2.78	–	6.42	71.18	1.94	–	–	99.78
11	17.93	1.09	7.38	–	6.44	65.34	–	–	1.90	100.08
12	17.19	–	–	–	6.40	74.62	1.28	–	–	99.49
Average	17.22	0.27	2.05	0.16	6.26	72.29	0.91	0.38	0.32	99.86
(apfu)	5.99	0.05	0.36	0.03	0.96	7.47	0.09	0.04	0.02	15
SD (σ)	0.256	0.284	1.855	0.118	0.262	2.795	0.468	0.491	0.021	

Note: – below detection limits (<~0.3 wt.%); (apfu) atoms per formula unit; EPMA — EDS-analytical system.

Arsenopyrite is a rare mineral. It occurs in small idiomorphic crystals in association with galena, sphalerite, jamesonite, and quartz. It is replaced by pyrite. Gersdorffite, also rare, often occurs as inclusions in sulfides or as regular square, hexagonal or octagonal shaped small crystals embedded in a quartz matrix. EPMA yielded following average chemical composition: $(Ni_{0.82},Fe_{0.14},Co_{0.03})_{\sum 0.99}(As_{0.93},Sb_{0.07})_{\sum 1.00}S_{1.01}$.

6.2. Sulfosalts

Berthierite, the only iron–sulfantimonite mineral so far identified in the Čumavići deposit, occurs in needle–like to prismatic crystals forming interlaced lenticular or nest–like aggregates (Fig. 3 l). Berthierite sometimes appears to have grown perpendicular to the cracks in a form of comb structures. Berthierite is most commonly intergrown with stibnite and sphalerite. Its lath–like crystals often replace sphalerite in a form of graphic intergrowths (Fig. 3 g, h). Berthierite also forms monomineralic ores with a breccia texture cemented with chalcedony. Cracks and fissures of berthierite aggregates were filled with kermesite, valentinite and senarmontite (Radosavljević et al., 1990). EPMA yielded following chemical composition for berthierite: $(Fe_{0.98},Mn_{0.04})_{\sum 1.02}Sb_{2.00}S_{3.99}$ (Table 2).

Lead–Sb-sulfosalts are the most abundant sulfosalts in the Čumavići deposit and throughout the SOF. The following seven mineral species were identified: geocronite, jamesonite, boulangerite, plagionite, semseyite, bournonite, and twinnite (Radosavljević and Dimitrijević, 2001; Rakić et al., 2003; Radosavljević et al., 2013). The Sb/Pb atomic ratio ranges from 0.3 to 2.0, mostly clustered in the range between 0.8 and 1.5 (boulangerite, semseyite, bournonite, jamesonite). Pb–Sb-sulfosalts occur in association with almost all ore minerals throughout mineralization sequence. They also form individual aggregates composed of prismatic, mm–cm-scale acicular and fibrous crystals (nm–μm) replacing older sulfides (Fig. 4d, e). These minerals were intimately intergrown with galena and sphalerite (Figs. 3i–k and 4f). The presence of polysynthetic twinning is characteristic for twinnite–guettardite. However, according to its optical and paragenetic features it most probably belongs to twinnite due to low As and high Sb contents. This mineral is identical to twinnite from the Sb–Pb–Zn–As Rujevac deposit (Moëlo, et al., 1983; Radosavljević, et al., 2014). EPMA of Pb–Sb sulfosalts are given in Tables 2 and 3.

The Pb–Ag–Sb-sulfosalts andorite and fizélyite were determined in the Čumavići deposit, but have not been observed elsewhere in the SOF. These minerals are relatively abundant and, locally, may be the principal carriers of Ag in the ore. Andorite, often intergrown with jamesonite, berthierite and rarely argyrodite, occurs as elongated or tabular aggregates. It is surrounded by stephanite and Ag–bearing tetrahedrite. Its bireflectance ranges between white–gray to blue–gray, and is characterized by red internal reflections. Andorite has higher reflectance than jamesonite and compared to galena, has approximately the same luster with bluish tint (Radosavljević et al., 1986). EPMA yielded the following average chemical composition: $Pb_{0.98}(Ag_{0.96},Fe_{0.08})_{\sum 1.04}Sb_{2.98}S_{6.02}$ (Tables 2 and 3).

Cu–Ag–Sb-sulfosalts are less widespread in the SOF. Argentian tetrahedrite, of varying composition, was determined in the Čumavići deposit. It often occurs in association with Ag–minerals, on grain boundaries of chalcopyrite and pyrite aggregates, or as individual grains embedded in quartz matrix. Cu–Ag–Sb-sulphosalts are crosscut by Pb–Sb

Table 5
Average EPMA of different generations of sphalerite and Pb–Sb-bearing sphalerite II and III from the Čumavići deposit, with apfu and CV (in wt.%).

Types of sphalerites	(n)	S	Mn	Fe	Cu	Zn	As	Cd	Sn	Sb	Pb	Total	Sb/Pb (apfu)
(Zn,Fe)S I	(12)	33.33	0.52	9.85	0.20	55.13	–	0.09	0.10	0.04	0.63	99.89	–
(apfu)		1.001	0.009	0.170	0.003	0.812	–	0.001	0.001	–	0.003	2	
Cv (%)		2	48	12	332	3	–	82	125	–	30		
(Zn,Fe)S II	(10)	32.82	0.35	5.88	0.03	59.87	0.05	0.03	–	0.16	0.54	99.73	0.5
(apfu)		0.995	0.006	0.102	–	0.891	0.001	–	–	0.001	0.003	2	
Cv (%)		2	39	15	–	3	–	–	–	–	107		
(Zn,Fe)S III	(53)	32.43	0.01	1.36	0.02	63.56	0.01	0.43	0.01	0.31	1.75	99.89	0.3
(apfu)		0.999	–	0.024	–	0.960	–	0.004	–	0.003	0.009	2	
Cv (%)		1	3592	71	503	2	–	93	725	91	28		
Average	(75)	32.63	0.14	3.32	0.05	61.72	0.01	0.32	0.02	0.24	1.41	99.86	0.3
(apfu)		0.999	0.002	0.058	0.001	0.927	–	0.003	–	0.002	0.007	2	
Cv (%)		2	334	102	881	5	1061	127	453	135	34		
(Pb + Sb)›ZnS II + III	(24)	32.20	0.01	1.44	0.03	62.65	0.02	0.54	–	0.72	2.32	99.93	0.5
(apfu)		0.999	–	0.025	–	0.953	–	0.005	–	0.006	0.011	2	
Cv (%)		1	–	93	488	3	–	84	–	47	18		

Note: (n) number of analyses; – not detected (< ~0.3 wt.%); (apfu) atoms per formula unit; Cv coefficient of variation (in %); EPMA — EDS-analytical system.

sulfosalts mainly jamesonite and semseyite (Fig. 5c). EPMA yielded the following chemical compositions: i) Ag(Au)–bearing tetrahedrite $(Ag_{5.80},Cu_{4.11},Au_{0.11})_{\sum 10.02}(Fe_{1.73},Zn_{0.28})_{\sum 2.01}Sb_{4.01}S_{12.95}$ (Table 2); ii) Ag(Fe)–bearing tetrahedrite $(Cu_{7.22},Ag_{2.74})_{\sum 9.96}Fe_{2.00}Sb_{4.02}S_{13.03}$ (Table 2); iii) Ag(Zn)–bearing tetrahedrite $(Cu_{8.07},Ag_{1.80})_{\sum 9.87}(Zn_{1.64},Fe_{0.41})_{\sum 2.05}Sb_{4.05}S_{13.03}$ (Table 2); iv) Ag(Bi)–bearing tetrahedrite $(Cu_{6.67},Ag_{3.29})_{\sum 9.96}(Fe_{1.80},Zn_{0.35})_{\sum 2.15}(Sb_{3.92},As_{0.07},Bi_{0.05})_{\sum 4.04}S_{12.85}$ (Table 3).

Silver–(Bi)–bearing tetrahedrite from the Čumavići deposit was described by Radosavljević et al. (1986). Almost all argentian tetrahedrite studied here show variable contents of Zn (<0.3–6.11 wt.%), Fe (1.32–6.27 wt.%), Ag (10.60–33.44 wt.%), and Au (<0.3–2.23

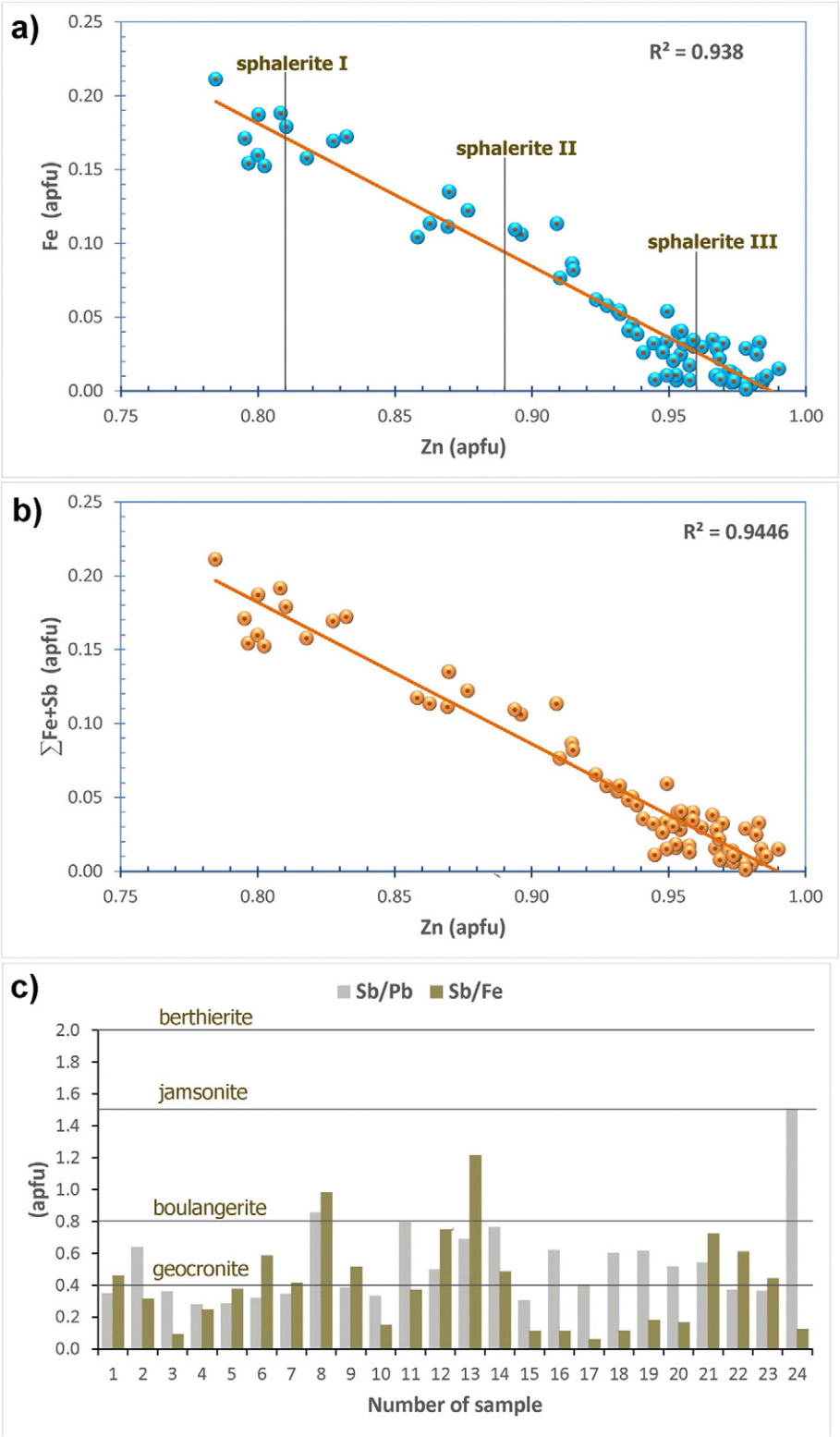

Fig. 6. Chemical variation of sphalerite expressed as a) Zn vs. Fe for the three generations of sphalerite; b) Zn vs. ∑Fe + Sb for sphalerite II and III; c) Sb/Fe and Sb/Pb atomic ratios in sphalerite II and III compared to those from Pb(Fe)–Sb sulfosalts; (apfu) – atoms per formula unit.

Table 6
The correlation matrix between macro and micro elements in sphalerite of all three generations according to atoms per formula unit (apfu) (75).

R^2	Fe	Cu	Zn	Cd	Sb
Cu	−0.231				
Zn	−0.968	0.084			
Cd	−0.710	0.229	0.657		
Sb	−0.294	0.446	0.236	0.366	
Pb	−0.332	0.114	0.272	0.366	0.466
∑Fe + Sb			−0.972		

Note: (n) number of analyses.

wt.%). Ag/(Ag + Cu) and Fe/(Fe + Zn) ratios range from 0.2 to 0.6 and from 1.0 to 0.2, respectively.

Ag–Sb-sulfosalts are widespread in the SOF, predominantly in the Northern and Northwest ore systems. Stephanite, polybasite, and pyrargyrite were observed in the Čumavići deposit. Compared to andorite, stephanite is an extremely rare Ag–bearing mineral in the deposit. Fine–grained stephanite often occurs with andorite and is accompanied by polybasite and Ag–bearing tetrahedrite. Needle–like intergrowths of stephanite with andorite and argyrodite were also observed (Fig. 5d). Stephanite is characterized by moderate light–pink to dark–reddish bireflectance. Pyrargyrite most commonly occurs along with quartz in fissures (Fig. 5e). Polybasite, usually intergrown with other sulfides and sulfosalts, is dull gray–white with no distinct pleochroism and moderate anisotropy. Dark red internal reflections are noticeable only in oil. EPMA yielded the following mean mineral compositions: pyrargyrite $(Ag_{2.69},Cu_{0.20},Fe_{0.08},Cd_{0.04})_{\Sigma 3.01}Sb_{0.98}S_{3.00}$ (Table 2); polybasite $(Ag_{14.97},Cu_{0.97},Zn_{0.03},Fe_{0.02})_{\Sigma 15,99}(Sb_{1.92},Bi_{0.18})_{\Sigma 2.10}S_{10.92}$ (Table 3); stephanite $(Ag_{4.84},Cu_{0.12},Fe_{0.01},Zn_{0.01})_{\Sigma 4.98}(Sb_{1.03},As_{0.16})_{\Sigma 1.19}S_{3.84}$ (Table 3).

Germanium–Ag sulfosalts are rare minerals in polymetallic deposits worldwide (Wang, 1978; Kuhs et al., 1979; Onoda et al., 1999; Paar et al., 2004). Argyrodite was determined in the Čumavići deposit for the first time in the present study. This mineral accompanies Cu–Ge–Ag–Au mineral associations in the form of isometric trapezoidal or rectangular grains (Fig. 5f). Argyrodite occurs also rarely in up to 100 μm–sized elongated aggregates, in which andorite forms rims on acicular crystals of stephanite (Fig. 5e). The luster of argyrodite is moderate, similar to argentian tetrahedrite. Very weak bireflectance with gray–pink to dirty–pink effects is noticeable. Argyrodite crystals with increased Au content have gray–purple to dark gray bireflectance. Anisotropy is weak; hardness is low, but slightly higher than galena and significantly lower than Ag(Fe)–tetrahedrite. EPMA data shows small amounts of Cu (up to 4.05 wt.%), Cd (up to 2.63 wt.%), Zn (up to 0.73 wt.%), and Fe (up to 1.09 wt.%) and the following mean composition: $(Ag_{7.47},Cu_{0.36},Cd_{0.09},Fe_{0.05},Zn_{0.03},Au_{0.02})_{\Sigma 8.02}(Ge_{0.96},In_{0.04})_{\Sigma 1.00}S_{5.99}$ (Table 4).

Argyrodite from the Čumavići deposit contains significant amounts of In (up to 1.80 wt.%), an economically important element throughout the SOF that is more usually present in sphalerite I (Table 3). From the calculated chemical formula for argyrodite, In would appear to substitute for Ge.

6.3. Native metals

Both native gold and native silver were determined in the Čumavići deposit. Native gold occurs only within Ag(Au)–Ge and Ag–Pb–Sb sulfosalts in association with chalcopyrite, arsenopyrite, marcasite, and pyrite. It also occurs as isolated grains (up to 10 μm) within a quartz matrix (Fig. 5 g). EPMA yielded the following chemical composition $(Au_{0.91},Ag_{0.09})_{\Sigma 1.00}$ (four analyses). Native silver is rare and occurs as exsolutions within argentian tetrahedrite.

6.4. Tungstates

Hübnerite is present in minor amounts, unevenly distributed in the deposit. It occurs in association with sphalerite, berthierite and quartz as thin, elongated crystals up to several cm in size which are commonly brecciated and cemented by quartz. Hübnerite was first mentioned by Kubat (1963), and later described in detail by Bermanec et al. (1988). EPMA of hübnerite yielded the chemical formula $(Fe_{0.62},Mn_{0.38},Ca_{0.03})_{\sum 1.03}WO_4$.

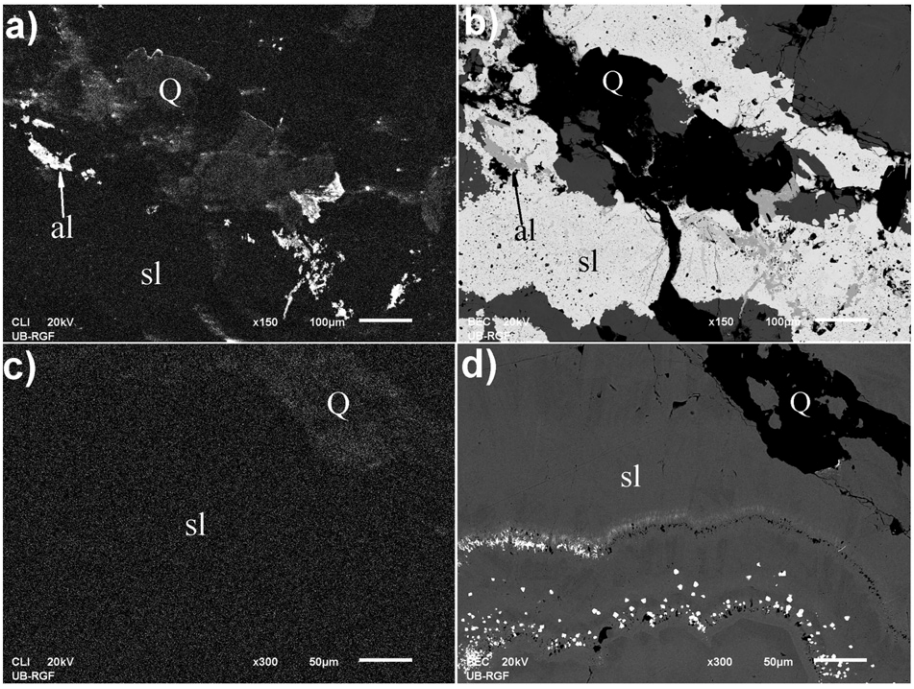

Fig. 7. SEM cathode mode images (a, c) and the same BSEI motif (b, d): a) strong cathodoluminescence corresponds to anglesite, weaker to quartz, while sphalerite aggregates do not display any cathodoluminescence effect, c) weak cathodoluminescence corresponds to quartz, sphalerite aggregates do not display any cathodoluminescence. Abbreviations: al — anglesite, Q — quartz, sl — sphalerite.

6.5. Gangue minerals

The main gangue minerals are quartz, chalcedony, and carbonates [Mn–siderite $(Mn_{0.59},Fe_{0.36},Ca_{0.04},Mg_{0.01})_{\sum 1.00}CO_3$ and rhodochrosite $(Mn_{0.88},Fe_{0.08},Ca_{0.04},Cu_{0.01})_{\sum 0.99}CO_3$; the average Fe/Mn atomic ratio in Mn-siderite and rhodochrosite is 0.61, and 0.09, respectively].

7. Sphalerite chemistry

EPMA trace and minor element data for various generations of sphalerite from the Čumavići deposit are shown in Tables 3 and 5. Sphalerite shows significant variation in the content of Mn (up to 2.18 wt.%), Fe (up to 12.12 wt.%), Cd (up to 1.48 wt.%), Cu (up to 1.56 wt.%), Sn (up to 0.53 wt.%), In (up to 0.11 wt.%), As (up to 0.54 wt.%), Sb (up to 1.62 wt.%), and Pb (up to 3.08 wt.%). Gallium, Ge, Ag, and Bi were below detection limits (<0.3 wt.% EDS, <0.01 wt.% WDS).

The content of minor elements in sphalerite I, obtained by MSA are (in ppm): Be = 6, B = 2, F = 5, Na = 80, Al = 50, Si = 80, P = 20, Cl = 300, K = 1000, Ti = 70, V = 1, Cr = 40, Co = 30, Ga = 2, Rb = 4, Sr = 30, Y = 1, Ag = 90, In = 8, Sn = 500, Sb = 200, W = 20, Bi = 0.1, Th = 0.01. Lithium, Mg, Sc, Ba, Hg and Tl were determined qualitatively. Germanium, Se, Br, Zr, Nb, Mo, Ru, Rh, Pd, Te, I, Cs, REE, Hf, Ta, Re, Os, Ir, Pt, Au, and U were not detected. Calcium, Mn, Cu, Zn, As, Pb and Cd concentrations are >0.1 wt.%. MSA data were normalized to Fe content of 9.59 wt.% (obtained by AAS).

The Na/K atomic ratio in sphalerite I at the Čumavići deposit is 0.14, similar to other sphalerite throughout the SOF (always <1) (Radosavljević, 1988). It should be emphasized that the alkali metals most probably occur in the form of sub-μm-scale daughter minerals within fluid inclusions.

Minimum and maximum values of atomic ratios in sphalerite of all three generations yielded the following chemical composition: $(Zn_{0.78-0.99},Fe_{<0.01-0.21}, Mn_{<0.01-0.04},Cu_{<0.01-0.02},Pb_{<0.01-0.01},Cd_{<0.01-}$

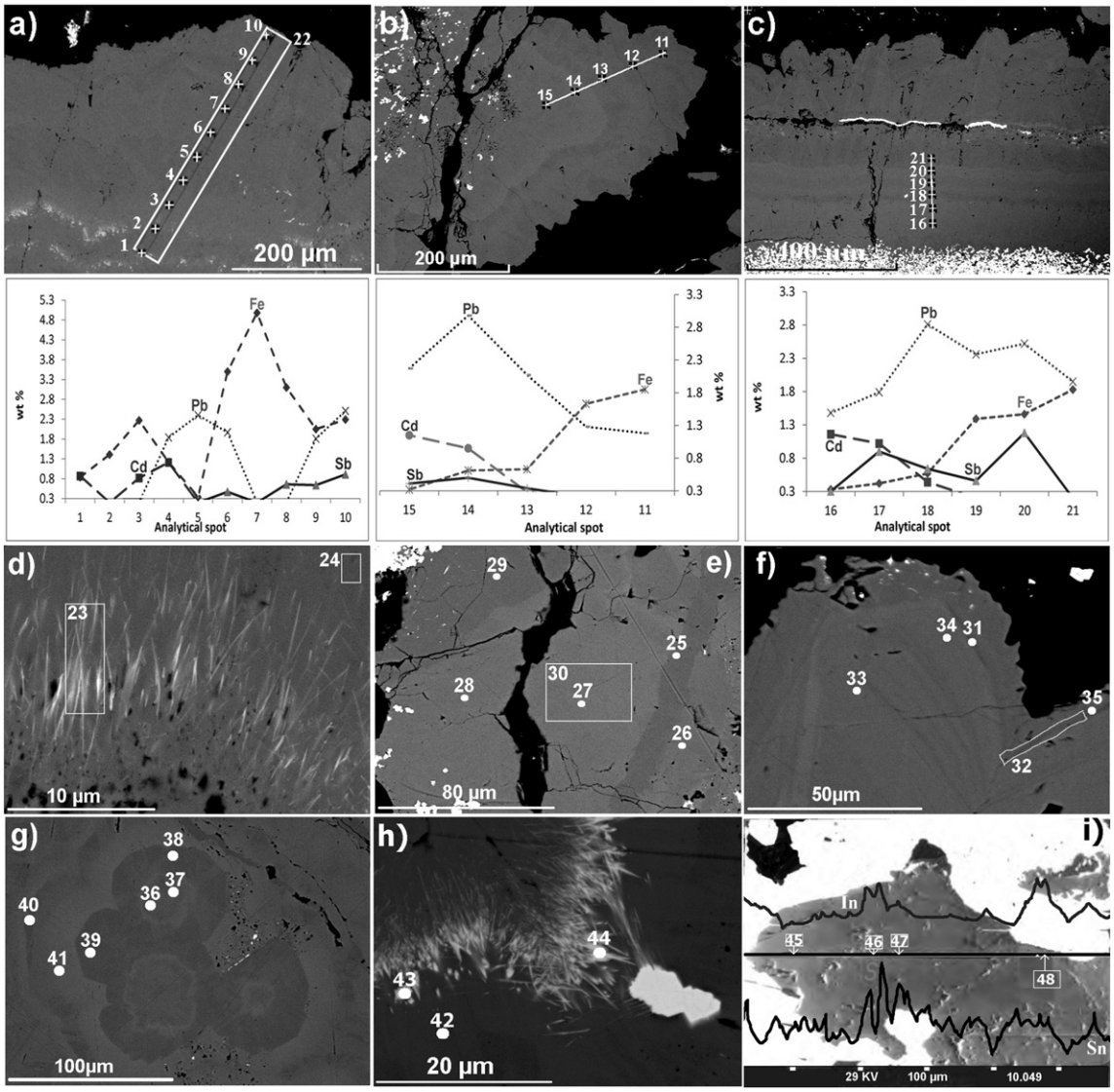

Fig. 8. Spot, area, and line EPMA of minor and trace elements in sphalerite of different generations (see also Table 7): a–c) spot-line analyses of Pb–Sb zones in sphalerite I and II accompanied by the related graphs of Fe, Cd, Sb, and Pb distribution; d) area analyses of Pb–Sb sulfosalt fibers and a sulfosalt–free sphalerite surface (sphalerite III); e) spot and area analyses of different zones of two generations of sphalerite (darker zones belong to sphalerite I (analytical spots 25 and 29), a lighter zones belong to sphalerite III); f) spot and area analyses of all three generations of sphalerite (lighter areas belong to sphalerite I corresponding to an increased content of Cu and Sn); g) Compositional variation across colloform–zoned sphalerite III (lighter areas correspond to an increased contents Cd, Sb, and Pb); h) spot analyses of Pb–Sb sulfosalt fibers and a sulfosalt–free sphalerite surface (sphalerite III); i) line analysis of InKα and SnKα in sphalerite I (gray) in association with galena (white) and quartz (black) (BEI + line WDS).

$_{0.01}$,$Sb_{<0.01-0.01}$)$\sum_{0.97-1.03}S_{0.97-1.03}$ (indium is below 0.001). The chemical formula of sphalerite I, II and III is as follows (Table 5):

- sphalerite I ($Zn_{0.812}$,$Fe_{0.170}$,$Mn_{0.009}$,$Cu_{0.003}$,$Pb_{0.003}$,$Cd_{0.001}$,$Sn_{0.001}$) $\sum_{0.999}S_{1.001}$;
- sphalerite II ($Zn_{0.891}$,$Fe_{0.102}$,$Mn_{0.006}$,$Pb_{0.003}$,$Sb_{0.001}$,$As_{0.001}$)$\sum_{1.005}S_{0.995}$;
- sphalerite III ($Zn_{0.960}$,$Fe_{0.024}$,$Pb_{0.009}$,$Cd_{0.004}$,$Sb_{0.003}$,)$\sum_{0.999}S_{0.999}$.

The content of trace– and minor–elements in sphalerite is in the following order: Fe > Pb > Cd > Sb > Mn > Sn > As > In. Variations of trace– and minor–elements in sphalerite occur along growth zones (Figs. 7d and 8a), and along colloform (Fig. 8b, c), needle–like (Fig. 8d), and/or fibrous textures (Fig. 8 h).

Table 7
EPMA of micro-elements in sphalerite and sulfosalts from Fig. 8 (in wt.%).

EDS	1	2	3	4	5	6	7	8	9	10	11
Mn	–	–	–	–	–	–	–	–	–	–	–
Fe	0.84	1.41	2.27	1.22	0.34	3.50	4.98	3.10	2.55	2.29	1.85
Cu	–	–	0.41	–	–	–	–	–	–	–	–
Cd	0.87	–	0.82	1.21	–	–	–	–	–	–	–
Sn	–	–	–	–	–	–	–	–	–	–	–
Sb	–	–	–	–	–	0.47	–	0.66	0.64	0.91	–
Pb	–	–	–	1.84	2.40	1.97	–	–	1.81	2.51	1.18
Sb/Pb (apfu)	–	–	–	–	–	0.4	–	–	0.6	0.6	–
Sulfosalts	/	/	/	/	/	G	/	/	F	F	/
EDS	12	13	14	15	16	17	18	19	20	21	22
Mn	–	–	–	–	–	–	–	–	–	–	–
Fe	1.63	0.63	0.61	0.32	0.33	0.42	0.57	1.39	1.46	1.83	2.30
Cu	–	–	–	–	–	–	–	–	0.26	–	–
Cd	–	0.28	0.95	1.15	1.16	1.02	0.44	–	0.26	–	0.45
Sn	–	–	–	–	–	–	–	–	–	–	–
Sb	–	0.34	0.50	0.41	0.30	0.90	0.64	0.46	1.18	–	–
Pb	1.28	2.07	2.98	2.17	1.48	1.79	2.81	2.36	2.52	1.95	1.34
Sb/Pb (apfu)	0.3	0.3	0.3	0.3	0.9	0.4	0.3	0.8	–	–	0.7
Sulfosalts	G	G	G	G	S	G	G	B	/	/	F
EDS	23	24	25	26	27	28	29	30	31	32	33
Mn	–	–	0.64	–	–	–	0.59	–	–	–	–
Fe	2.19	1.70	6.30	0.74	0.43	0.36	6.45	0.59	9.16	9.06	3.30
Cu	–	–	–	–	–	–	–	–	1.56	0.58	–
Cd	–	–	–	0.69	1.29	1.48	–	1.43	0.20	–	–
Sn	–	–	–	–	–	–	–	–	0.28	0.39	–
Sb	2.48	–	–	–	–	0.48	–	0.57	–	–	–
Pb	6.01	–	–	2.31	2.02	2.20	–	2.66	2.00	1.67	1.8
Sb/Pb (apfu)	–	–	–	–	–	0.4	–	0.4	–	–	–
Sulfosalts	/	/	/	/	/	G	/	G	/	/	/
EDS	34	35	36	37	38	39	40	41	42	43	44
Mn	–	–	0.10	–	–	–	–	–	–	–	–
Fe	0.57	6.54	0.41	0.40	0.51	0.43	3.11	1.15	1.80	0.96	0.59
Cu	–	0.33	–	–	–	–	–	–	–	–	–
Cd	0.38	–	1.26	1.16	0.38	0.84	–	0.35	–	–	–
Sn	0.25	–	–	–	–	–	–	–	–	–	–
Sb	–	–	0.67	1.06	–	–	–	1.22	0.44	16.5	20.22
Pb	–	1.21	2.28	2.62	1.74	–	1.69	2.71	2.44	37.6	45.69
Sb/Pb (apfu)	–	–	0.5	0.7	–	–	–	0.8	0.3	0.7	0.8
Sulfosalts	/	/	G	F	/	/	/	B	G	F	B
WDS	45	46	47	48							
Mn	0.08	0.06	0.14	0.08							
Sn	0.40	0.61	0.32	0.70							
In	0.01	0.07	0.01	0.11							

Note: EDS — analytical system; WDS — analytical system; – below detection limits (<~0.3 wt.% for EDS and <~0.01 for WDS); (apfu) atoms per formula unit; possible Pb–Sb sulfosalts according to Sb/Pb (apfu): G geocronite (0.4), F falkmanite (0.7), B boulangerite (0.8), S semseyite (0.9); / undefined.

Table 8
XRPD data for sphalerite and galena from Čumavići.

Sample characterization		
Name (chemical, mineral)		Sphalerite/galena
Empirical formula		ZnS/PbS
Source/preparation		Natural mineral
Technique		
Radiation type, source	X-rays, Cu λ value used 1.54060 Å $K\alpha_1$/1.54439 $K\alpha_2$	
Monochromator	diffracted beam graphite monochromator	
Detector (film, scint. etc.)	Proportional	
Instrument description (type, slits)	Vertical diffractometer Divergence slit 1° Receiving slit 0.1 mm Soller slit 1°	
Instrumental profile breadth	0.10 °2θ temp. (°C) 25 ± 1	
Specimen form/particle size	Edge loaded powder/ <10 μm particle size	
Range of 2θ	From 4 to 80 °2θ	
Specimen motion	None	
Unit-cell data	**Sphalerite**	**Galena**
Unit-cell parameters	$a = 5.412(1)$Å, $V = 158.49(9)$Å^3, $Z = 4$, $D_x = 4.08$ g/cm^3	$a = 5.934(1)$Å, $V = 209.0(1)$Å^3, $Z = 4$, $D_x = 7.60$ g/cm^3
Formula wt.	97.47 g/mol	239.27 g/mol
Crystal system	Cubic	Cubic
Space group	$F\bar{4}3m$ (216)	$Fm\bar{3}m$ (225)

Three major groups of sphalerite are distinguished on the basis of Fe content, corresponding to the previously defined mineralization stages (Fig. 6a). A correlation analysis was carried out in order to determine major and minor–elements and their interrelationships.

In addition, a nearly perfect Sn vs. In correlation ($R^2 = 0.975$), and a strong negative Sn vs. Mn correlation ($R^2 = -0.722$) was determined in sphalerite I. Also, a good negative Fe vs. Cd and positive Zn vs. Cd correlation (Table 6, Fig. 6b) were determined in all three sphalerite generations. It should be emphasized that a Sb vs. Cu correlation ($R^2 = 0.446$) has not been determined suggesting that Sb is not incorporated in the crystal structure of sphalerite via coupled substitution (e.g., $2Zn^{2+} \leftrightarrow Cu^{+} + Sb^{3+}$), but present as micro–inclusions of sulfosalts. Contrary to this, an excellent correlation between the Cu and In in Cu–In-bearing sphalerite offers indirect proof for the coupled substitution $2Zn^{2+} \leftrightarrow Cu^{+} + In^{3+}$, which allows indium to enter the sphalerite structure (Cook et al., 2012).

On the basis of Sb and Pb contents, there are light areas in sphalerite II and III containing only Pb (most commonly), both elements, and/or without both elements (Tables 3 and 5, Fig. 8a–c). Lead–Sb-bearing sphalerite is usually Fe-poor (II and III generation). The Sb/Pb atomic ratio varies in the range from 0.3 to 1.5, similarly to ratios corresponding to geocronite and jamesonite (Fig. 6c), suggesting the presence of submicroscopic inclusions of the above sulfosalts in sphalerite. It is also possible that part of the submicroscopic sulfosalts is in the form of stibnite, indicated by the ideal negative Zn vs. ∑Fe + Sb correlation

Table 9
Comparison of calculated and observed XRPD data of galena and sphalerite from Čumavići.

h k l	I_{rel} (%)	Galena		Sphalerite		I_{rel} (%)
		$d_{(obs)}$ (Å)	$d_{(calc)}$ (Å)	$d_{(obs)}$ (Å)	$d_{(calc)}$ (Å)	
1 1 1	37	3.4308	3.4262	3.1248	3.1245	88
2 0 0	56	2.9626	2.9672	2.7059	2.7059	11
2 2 0	36	2.0962	2.0981	1.9133	1.9133	67
3 1 1	20	1.7888	1.7893	1.6317	1.6317	8
2 2 2	8	1.7139	1.7131	1.5607	1.5622	40
4 0 0	6	1.4835	1.4836	1.3523	1.3529	5
3 3 1	5	1.3624	1.3614	1.2418	1.2415	11
4 2 0	10	1.3273	1.3270	1.2108	1.2101	9
4 2 2	9	1.2110	1.2113	–	–	–

Table 10
Dependence of the *a* unit–cell parameter on FeS portions (mol%) in sphalerite from Čumavići in comparison to literature data (FeS portions in sphalerite of this study was calculated).

Literature	Kullerud (1953)					This study
a (Å)	5.424	5.421	5.419	5.417	5.415	5.412(1)
FeS (mol.%)	41.4	34.2	27.9	22.4	17.5	9.2

(Fig. 6b). Berthierite was not detected within Pb–Sb-bearing sphalerite with Sb/Fe atomic ratio up to 1.2 (Fig. 6c).

The Pb–Sb-bearing sphalerite does not display effects of cathodoluminescence (Fig. 7a, c). Quartz veinlets show weak, while anglesite displays strong effects of cathodoluminescence (Fig. 7a). This somewhat confirms the hypothesis that most of the Sb and Pb in sphalerite is related to submicroscopic Pb–Sb sulfosalt inclusions. Besides Pb, Sb, and Pb–Sb in sphalerite we also detected in Fe–rich sphalerite I, zones enriched in Cu and Sn (Fig. 8f, Table 7), and In and Sn (Fig. 8i, Table 7).

The absence of correlation of Pb with other elements confirms the hypothesis that lead in sphalerite is related to the presence of submicroscopic galena and sulfosalts inclusions. In an analogous study, Pačevski et al. (2012) concluded on the basis of TEM and EPMA data that Pb–bearing pyrite from the Čoka Marin Cu–Pb–Zn–Au deposit, Serbia, can be attributed to nano–inclusions (<50 nm) of sulfosalts of Pb-(±As, Ag, Cu).

8. X-ray powder diffraction analysis

X–ray powder diffraction (XRPD) was used for identification and calculation of unit–cell parameters of sphalerite (III generation) and galena from Čumavići deposit. Results are presented in Tables 8–10. XRPD data of the analyzed sphalerite and galena are given in Table 8 and a comparison between calculated and observed XRPD data of sphalerite and galena are shown in Table 9. In comparison to the published unit-cell parameter data for sphalerite (Kullerud, 1953) of, the analyzed sample from the Čumavići deposit belongs to a Fe–poor variety (Table 10, Fig. 9). Literature unit–cell data for sphalerite show an ideal linear dependence, which can be calculated by the equation $y = 5.40861 + 0.00037 \cdot x$. According to this, the FeS portion and other minor– and trace–elements in analyzed sphalerite amounts to 9.2 mol%. The unit–cell parameter of galena is in excellent agreement with the literature data (JCPDS card no. 05-0592, 1953; Noda et al., 1987; Noda et al., 1983; Berger et al., 1985; Faizullina et al., 1983a,b). The dependence of the *a* unit–cell parameter on FeS portions (mol%) in sphalerite from Čumavići in comparison to the literature data are given in Table 10 and Fig. 9.

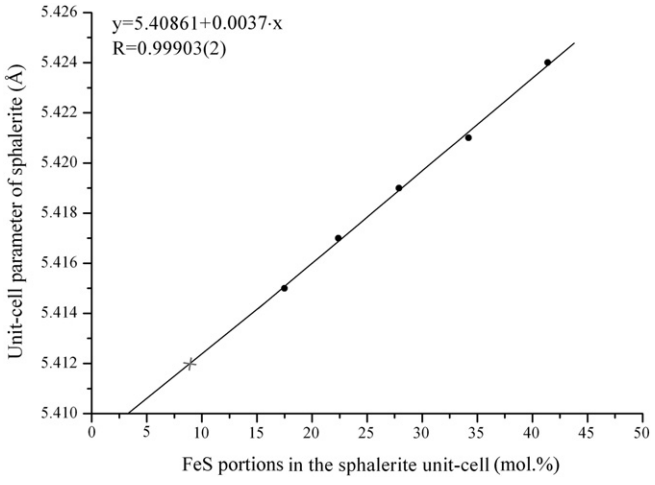

Fig. 9. Dependence of the *a* unit–cell parameter on mol% FeS in sphalerite III from Čumavići (black dots–literature data (Table 10), the red cross marks the position of the sphalerite III unit–cell *a* parameter of the analyzed sample).

9. Discussion

9.1. Micro and trace element distributions in sphalerite

Antimony and lead in the studied sphalerite are in the form of isometric or fibrous micro– to nano–scale inclusions of Sb–Pb-bearing minerals. Furthermore, Sb and Pb are in the form of thin wavy ribbons composed of galena or Pb–Sb sulfosalts. These textural combinations are numerous in sphalerite II and III (Fig. 7d). Cook et al. (2009), analyzed sphalerite from 26 deposits worldwide, similarly concluded that elevated Pb, Sb, and Bi contents in sphalerite were the result of micro– to nano–scale inclusions, and not of isomorphous substitution in the crystal structure. However, minor amounts of Sb and Pb likely substituted for Zn^{2+} in the sphalerite structure, as can be postulated by the form (and chemistry) of different bright zoned areas (Figs. 3b and 8a–c, e). These effects are also visible in reflected light, regularly as rhythmic bands with numerous yellow to reddish internal reflections (in oil, Fig. 3i–k). Similar reddish effects were observed in sphalerite from the Au–Cu polymetallic deposits Palai-Islica (Spain) (Carrillo-Rosua et al., 2008). Different types of sphalerite have significant amounts of minor and trace elements, such as Cu (up to 1.34 at.%), Sb (up to 0.67 at.%), Sn (up to 0.31 at.%), Ge (up to 0.29 at.%), Cd (up to 0.24 at.%), In (up to 0.18 at.%), Mn (up to 0.15 at.%) and Ga (up to 0.12 at.%). Among them, Sb, Sn, Ga, Ge and In are proportional to Cu content, and the following charge–balanced coupled substitutions have been demonstrated: $Sb^{3+} + Cu^{+} + Cu^{2+} \leftrightarrow 3Zn^{2+}$; $Sn^{4+} + 2Cu^{+} \leftrightarrow 3Zn^{2+}$; $2Ge^{2+} + Ga^{3+} + 2Cu^{2+} + Cu^{+} \leftrightarrow 6Zn^{2+}$ (Carrillo-Rosua et al., 2008). Moreover, increasing intensity of color of sphalerite from the Force Crag Pb–Zn deposit, England, depends on the enrichment in Cu, Fe, Sb, Ag, and Pb (Dickinson and Pattrick, 1987). TEM studies revealed these trace–element–rich zones of sphalerite contained precipitates of tetrahedrite–like composition, and are a possible cause of the coloration in sphalerite. However, similar color bands enriched in Cu, Sb, Ag, and Pb occurring in colloform sulfides from the Silvermines orebody, Ireland, was found to be devoid of precipitates, suggesting in this case, the accommodation of these trace elements into sphalerite structure (Dickinson and Pattrick, 1987). In addition, Maslennikov et al. (2009) confirmed that Sb, As, and Pb enrichment in sphalerite is attributed to submicroscopic galena-tetrahedrite inclusions, whereas the Co and Mn likely substitute for Zn^{2+} in the structure. According to Ye et al. (2011) LA–ICP–MS time-resolved depth profiles for sphalerite from a number of Chinese deposits confirm the presence of elements such as Co, In, Ge, Ga, and Cd in solid solution, and also that Ag, Sn, Tl, and Sb are likely present within the crystal structure.

SEM spot and line profile analyses of Pb–Sb-bearing sphalerite from the Čumavići deposit confirmed that there is no regularity in the occurrence of Pb and Sb. These elements concentrate in light areas, above and below visible parallel wavy ribbons accompanied with galena and Pb–Sb sulfosalts (Fig. 8a–c). These zones are usually composed of several rhythmic bands (lighter and darker), where bands closer to the center are enriched with galena, while those peripheral are enriched in Pb–Sb sulfosalts. Zones enriched in Fe and variable content of Sb were found along sphalerite aggregate boundaries (Fig. 8a–c). Finally, increased amounts of Mn, Cu, Sn, and In, as well as of Cd, Sb, and Pb are characteristic for sphalerite I and for sphalerite II and III, respectively (Tables 3 and 5). Besides enrichment in Fe, Pb, Cd, Sb, Mn, Sn, As, and In, micro- to submicro-scale inclusions of quartz are also characteristic for Pb–Sb bearing sphalerite (black dots in Fig. 8d).

9.2. Variation in sphalerite composition within the Čumavići deposit

Sphalerite from the Čumavići deposit crystallized from medium– to low–temperature hydrothermal solutions, which were rapidly precipitated in faults and fissures within volcanic rocks. There are three generations of sphalerite: sphalerite I and sphalerite II corresponds to Fe-rich (12.0–19.2 and 4.7–8.4 mol% FeS, respectively), while sphalerite III are Fe–poor (0.3–3.8 mol% FeS). Colloform zoned areas occurring in central parts of Pb–Sb bearing sphalerite show tendency towards hexagonal forms (Fig. 8 g). This observation suggests possible initial crystallization of wurtzite from gels, which later recrystallized into sphalerite. Moreover, colloform textures of sphalerite aggregates point at recrystallization. Sphalerite I (Fig. 8e) is overgrown by colloform zones of Pb–Sb sphalerite II and III (Fig. 8 g) suggesting here that it was partly corroded, dissolved and remobilized by hydrothermal solutions. This supports the hypothesis that these solutions changed, with occasional influx of Fe and Pb–Sb.

Similar processes happened in several Pb–Zn–Cu–Sb deposits in Rheinisches Schiefergebirge (Germany). The oldest generation of sphalerite is overgrown by various Pb–Sb sulfosalts (Wagner and Cook, 1998). According to these authors, sulfosalt–rich solutions altered early sphalerite, thus newly creating Zn- and Fe-poor solutions, from which sphalerite II crystallized. In this way, various structural and textural modifications were formed, which further led to the complexity of ore deposition in the veins.

9.3. Environmental impact

Estimated ore reserves of the SOF are 50 million tonnes; the Čumavići deposit contains around 600,000 tonnes (Čobić, 1978). No mining currently takes place due to technological issues but the Čumavići deposit is considered a valuable future resource because of the rare and critical metal associations. Knowing the compositional variation present in sphalerite is of great importance since it is the main zinc source. Understanding the distribution of Pb and Sb in sphalerite will impact on mineral processing (e.g., flotation, gravity), and can help explain unsatisfactory results (Kubat, 1995). This is also the case for the Rujevac Sb(As)–Pb–Zn polymetallic deposit, where elevated Hg contents in sphalerite occur (Radosavljević et al., 2012). From the aspects of environmental protection, hydrometallurgy is probably the most suitable process for extraction of a large number of ore metals (Zn, Pb, Sb, Ag, Au etc.) from zinc concentrates. This issue will be the subject of future work.

10. Conclusions

1) Sphalerite, occurring in four generations in the SOF, was deposited from hydrothermal solutions over a wide temperature range from 400 to 100 °C (Dangić, 1982). Sphalerite that crystalized at the end of the hydrothermal process differs in chemical composition from the earlier generations, notably with respect to Fe content. High–temperature sphalerite contains from 15 to 22 mol% of FeS, and often has increased contents of Mn, Cu, Sn, and In. Sphalerite deposited at low temperatures has FeS contents from <1 to 5 mol%, and increased contents of Cd, Pb and Sb.
2) Sphalerite from Čumavići displays an extraordinary range of chemical composition. Significant amounts of Pb and Sb have been detected — between 0.10–3.08, and 0.02–1.62 wt.%, respectively. A large part of these elements are in the form of inclusions, while only a small part is substituted for Zn^{2+} in the crystal structure of (Pb–Sb)-bearing sphalerite (light zoned areas on the SEM images). These effects are also visible in reflected light, regularly as rhythmic bands with numerous yellow to reddish internal reflections.
3) Sphalerite has its own specifics within the SMMP. According to genetic and chemical composition, sphalerite from the SOF is the most similar to those from the Rogozna (Radosavljević et al., 2015) and Sasa orefields (Strmic-Palinkas et al., 2013). Sphalerite displays a range of genetic, paragenetic and geochemical characteristics across the PMD, and these differences are directly related to the different types of magmatism and lithological environments. In the SOF, ore–bearing solutions were generated from the Srebrenica intrusive–volcanogenic complex (Radosavljević et al., 2013), whereas in the BOF they originated from subvolcanic–plutonic intrusions of Boranja. Specific sphalerite compositions are a response to the local setting in which ore minerals were deposited. Unlike SOF, ore deposits within the BOF formed exclusively in silicate–carbonate–rich environments. In the BOF, sphalerite is associated with skarn and high–temperature hydrothermal substages, containing elevated FeS (up to 22 mol%), Mn and Cu; In and Sn are almost absent. Low–temperature sphalerite has increasing contents of Cd, Hg, As, In and Ga (Radosavljević et al., 2012).
4) Within the Ag–bearing tetrahedrite series, Ag content increases with elevated Fe/(Fe + Zn) atomic ratios, and is the highest in Au–bearing tetrahedrites. This regularity points to a high activity of Ag and Au in the low–temperature hydrothermal substage, when rare Ag–Pb–Sb, Ag–Sb, Ag(Au)–Cu–Sb and Ag(Au)–Ge sulfosalts were deposited. This mineral association is unique for the whole SOF because Au concentrations are of economic significance. The deposit represents a rare morphogenetic type of epithermal gold mineralization within the SMMP.

Acknowledgments

This paper presents results from Project OI-176016 (Magmatism and geodynamics of the Balkan Peninsula from Mesozoic to present day: significance for the formation of metallic and non-metallic mineral deposits), granted by the Ministry of Education, Science and Technological Development of the Republic of Serbia. The authors warmly thank our colleague Dr. Velizar Štrumberger for supplying the EPMA data. The authors express their deepest gratitude to our colleague Robert Kellie, consulting geologist, for proofreading of the manuscript. Critical reviews of the manuscript by Panagiotis Voudouris, Nigel Cook and an anonymous reviewer led to important modifications of the paper and are highly appreciated. We also acknowledge with thanks the editorial handling of our manuscript by Editor-in-Chief Franco Pirajno and Associate Editor Cristiana Ciobanu.

References

Anthony, J.W., Bideaux, R.A., Bladh, K.W., Nichols, M.C., 1990. Handbook of mineralogy. Elements, Sulfides, Sulfosalts vol. I. Mineral Data Publishing, Tucson, AZ, USA.
Arce-Burgoa, O., Goldfarb, R., 2009. Metallogeny of Bolivia. SEG Newsl. 79, 7–15.
Berger, H., Niebsch, H.H., Szczerbakow, A., 1985. Lattice parameters in the solid-solution system PbS_xSe_{1-x}. Cryst. Res. Technol. 20, K8–K10.
Bermanec, V., Radosavljević, S., Tibljaš, D., 1988. Wolframites from Srebrenica mine area. Proceedings of Scientific MeetingJournal of the National Museum. Department of Natural Sciences, Sarajevo, BiH, pp. 37–43 (in Croatian with English summary).
Borodaev, Y.S., 1978. Mineral associations in the system Pb–Sb–S on deposits of various types. Geol. Ore Deposits 20, 52–63 (in Russian).
Carrillo-Rosua, J., Morales-Ruano, S., Fenoll Hach-Ali, P., 2008. Textural and chemical features of sphalerite from the Palai-Islica deposit (SE Spain): implications for ore genesis and color. Neues Jb. Mineral. Abh. 185, 63–78.
Chvilyova, T.N., Bezsmertnaya, M.S., Spiridonov, E.M., Agroskin, A.S., Papayan, G.V., Vinogradova, R.A., Lebedeva, S.I., Zav'yalov, E.N., Filimonova, A.A., Petrov, V.K., Rautian, L.P., Veshnikova, O.L., 1988. Manual — Determination of the Ore Minerals on Reflected-Light. NEDRA, Moscow (in Russian).
Čobić, T., 1978. Contribution to the knowledge of Srebrenica ore deposit. Proceedings, 9th Congress of Geologists of Yugoslavia. Sarajevo, pp. 555–564 (in Serbian with English abstract).
Cook, N.J., Ciobanu, C.L., Pring, A., Skinner, W., Shimizu, M., Danyushevsky, L., Saini-Eidukat, B., Melcher, F., 2009. Trace and minor elements in sphalerite: a LA-ICPMS study. Geochim. Cosmochim. Acta 73, 4761–4791.
Cook, N.J., Ciobanu, C.L., Brugger, J., Etschmann, B., Howard, D.J., de Jonge, M., Ryan, C.G., Paterson, D., 2012. Determination of the oxidation state of Cu in substituted Cu–In–Fe-bearing sphalerite via μ-XANES spectroscopy. Am. Mineral. 97, 476–479.
Cvetković, V., Prelević, D., Downes, H., Jovanović, M., Vaselli, O., Pecskay, Z., 2004. Origin and geodynamic significance of Tertiary postcollisional basaltic magmatism in Serbia (Central Balkan Peninsula). Lithos 73, 161–186.

Dangić, A., 1978. Geochemistry of Hydrothermal Alteration of the Rocks around the Sulfide Mineralization and Evolution of Hydrothermal Activity on the Example of Srebrenica and Kišnica (Dissertation), University of Belgrade, Serbia (in Serbian with English summary).

Dangić, A., 1982. Temperature, composition and evolution of the ore-bearing fluids in the Srebrenica area. Proceedings, 10th Congress of Geologists of Yugoslavia. Budva, pp. 67–79 (in Serbian with English abstract).

Dickinson, C.R., Pattrick, A.D., 1987. A TEM investigation of optical variations in sphalerite. Mineral. Mag. 51, 127.

Faizullina, N.R., Latypov, Z.M., Savel'ev, V.P., 1983a. Solid solutions based on PbS in the system Tl–Pb–S. Inorg. Mater. 19, 612–614.

Faizullina, N.R., Latypov, Z.M., Savel'ev, V.P., 1983b. Solid solutions based on PbS in the system Tl–Pb–S. Inorg. Mater. 19, 1587–1589.

Fontboté, L., Amstutz, G.C., Cardozo, M., Cedillo, E., Frutos, J., 1990. Stratabound ore deposits in the Andes. Special Publication of the Society for Geology Applied to Mineral Deposit vol. 8. Springer-Verlag, Berlin-Heidelberg.

Garvey, D., 1986. LSUCRIPC least squares unit cell refinement with indexing a personal computer. Powder Diffract. 1, 114.

George, L., Cook, N.J., Ciobanu, C.L., Wade, B.P., 2015. Trace and minor elements in galena: a reconnaissance LA–ICP–MS study. Am. Mineral. 100, 548–569.

Janković, S., 1990. The Ore Deposits of Serbia: Regional Metallogenetic Settings, Environments of Depositon, and Types. Faculty of Mining and Geology, Belgrade University (in Serbian with English summary).

Janković, S., Mozgova, N.N., Borodaev, Y.S., 1977. The complex antimony lead–zinc deposit at Rujevac/Yugoslavia; its specific geochemical and mineralogical features. Mineral. Deposita 12, 381–392.

Janković, S., Zarić, P., Radosavljević, S., 1992. Srebrenica: complex Pb–Zn–Ag–Sb–Sn ore field related to subvolcanic environment. Proceedings of 6th Congress Geological Society of Greece, Athena, IGCP, p. 262.

Karamata, S., Dimitrijević, D.M., Dimitrijević, N.M., Milovanović, D., 2000. A correlation of ophiolitic belts and oceanic realms of the Vardar zone and the dinarides. Proceedings of the International Symposium Geology and Metallogeny of the Dinarides and the Vardar Zone. Banja Luka, Bosnia and Herzegovina, pp. 191–194.

Keutsch, F., de Brodtkorb, M.K., 2008. Metalliferous paragenesis of the San José mine, Oruro, Bolivia. J. S. Am. Earth Sci. 25, 485–491.

Kouzmanov, K., Bailly, L., Tamas, C., Ivascanu, P., 2005. Epithermal Pb–Zn–Cu (–Au) deposits in the Baia Mare district, Eastern Carpathians, Romania. Box 1–2. Ore Geol. Rev. 27, 48–49.

Kubat, I., 1963. Hubnerite at the village Čumavići in East Bosnia. Geološki Glasnik, Sarajevo, Bosnia and Herzegovina 7, pp. 27–31 (in Serbian with English summary).

Kubat, I., 1995. Metallogeny antimony and mercury in Bosnia and Herzegovina and possibility to produce and process them. Geološki Glasnik, book XIII, Sarajevo, Bosnia and Herzegovina, pp. 1–164 (in Serbian with English summary).

Kuhs, W.F., Nitsche, R., Scheunemann, K., 1979. The argyrodites — a new family of tetrahedrally close-packed structures. Mater. Res. Bull. 14, 241–248.

Kullerud, G., 1953. The FeS–ZnS system. A geological thermometer. Nor. J. Geol. 32, 61–147.

Lehmann, B., Ishihara, S., Michel, H., Miller, J., Rapela, C., Sanchez, A., Tistl, M., Winkelmann, L., 1990. The Bolivian Tin province and regional Tin distribution in the Central Andes; a reassessment. Econ. Geol. 85, 1044–1058.

Maslennikov, V.V., Maslennikova, S.P., Large, R.R., Danyushevsky, L.V., 2009. Study of trace element zonation in vent chimneys from the Silurian Yaman-Kasy volcanic-hosted massive sulfide deposit (Southern Urals, Russia) using laser ablation–inductively coupled plasma mass spectrometry (LA–ICPMS). Econ. Geol. 104, 1111–1141.

Moëlo, Y., Borodaev, Y.S., Mozgova, N.N., 1983. The twinnite–zinkenite–plagionite association from the Sb–Pb–Zn deposit, Rujevac, Yugoslavia. Bull. Mineral. 106, 505–510 (in French with English summary).

Neubauer, F., 2002. Contrasting Late Cretaceus with Neogene ore provinces in the Alpine–Balkan–Carpathian–Dinaride collision belt. Geol. Soc. Lond., Spec. Publ. 204, 81–102.

Noda, Y., Ohba, S., Sato, S., Saito, Y., 1983. Charge distribution and atomic thermal vibration in lead chalcogenide crystals. Acta Crystallogr. B39, 312–317.

Noda, Y., Masumoto, K., Ohba, S., Saito, Y., Toriumi, K., Iwata, Y., Shibuya, I., 1987. Temperature dependence of atomic thermal parameters of lead chalcogenides, PbS, PbSe and PbTe. Acta Crystallogr. C43, 1443–1445.

Onoda, M., Chen, X.A., Kato, K., Sato, A., Wada, H., 1999. Structure refinement of Cu_8GeS_6 using X-ray diffraction data from a multiple-twinned crystal. Acta Crystallogr. B55, 721–725.

Paar, W.H., Roberts, A.C., Berlepsch, P., Armbruster, T., Topa, D., Zagler, G., 2004. Putzite, $(Cu_{4.7}Ag_{3.3})_8GeS_6$, a new mineral species, from Capillitas, Catamarca, Argentina: Description and crystal structure. Can. Mineral. 42, 1757–1769.

Pačevski, A., Moritz, R., Kouzmanov, K., Marquardt, K., Živković, P., Cvetković, Lj, 2012. Texture and composition of Pb-bearing pyrite from Čoka Marin polymetallic deposit, Serbia, controlled by nanoscale inclusions. Can. Mineral. 50, 1–20.

Petković, M., 1997. On magmatic complexes and metallogenetic affinity (an example from the Tethys Sea). Proceedings of Symposium "Ore Deposits Exploration". Faculty of Mining and Geology, Belgrade, Serbia, pp. 5–16.

Petković, M., Romić, K., 1980. Prognostication of endogenic deposits in the Srebrenica ore field. Transcripts of Faculty of Mininig and Geology, Belgrade 22, pp. 57–64 (in Serbian with English summary).

Picot, P., Johan, Z., 1982. Atlas of Ore Minerals. Elsevier, Amsterdam.

Pirajno, F., 1992. Hydrothermal Mineral Deposits. Principles and Fundamental Concepts for the Exploration Geologist. Springer-Verlag, Berlin-Heidelberg.

Powder Diffraction File, Card No. 05-0592, 1953. Joint Committee on Powder Diffraction Standards (JCPDS) Swarthmore, PA.

Prelević, D., Foley, S.F., Romer, R.L., Cvetković, V., Downes, H., 2005. Tertiary ultrapotassic volcanism in Serbia: constraints on petrogenesis and mantle source characteristics. J. Petrol. 46, 1443–1487.

Radosavljević, S., 1988. Nature of Silver in Pb–Zn Deposits of the Podrinje Metallogenic District: Mineralogy and Genetic Features (Dissertation), University of Belgrade, Serbia (in Serbian with English summary).

Radosavljević, S., Dimitrijević, R., 2001. Mineralogical data and paragenetic association for semseyite from srebrenica ore field, Bosnia and Herzegovina. Neues Jb. Mineral. Monat. 146–156.

Radosavljević, S., Rakić, S., Štrumberger, V., Dimitrijević, R., Cvetković, Lj., 1986. Minerals of silver from Pb–Zn deposits of the Podrinje metalogenic district. Proceedings, 11th Congress of Geologists of Yugoslavia. Tara, pp. 77–88 (in Serbian with English abstract).

Radosavljević, S., Dimitrijević, R., Cvetković, Lj, Stojanović, M., 1990. Berthierite from polymetallic deposit of Čumavići (Srebrenica). Proceedings of 12th Geological Congress of Yugoslavia, Ohrid, FYRM, pp. 810–818 (in Serbian with English summary).

Radosavljević, S., Rakić, S., Stojanović, J., Radosavljević-Mihajlović, A., 2005. Occurrence of Petrukite in Srebrenica Ore field, Bosnia and Herzegovina. Neues Jb. Mineral. Abh. 181, 21–26.

Radosavljević, S., Đorđević, D., Stojanović, J., Kašić, V., 2011. Srebrenica ore field, Podrinje Metallogenic District, East Bosnia: greisenization and mineralization of tin, titanium and REEs. Proceedings, 4th Consulting Geologists of Bosnia and Herzegovina, Sarajevo, BiH, pp. 117–126 (in Serbian with English summary).

Radosavljević, A.S., Stojanović, N.J., Pačevski, M.A., 2012. Hg-bearing sphalerite from the Rujevac polymetallic ore deposit, Podrinje Metallogenic District, Serbia: compositional variations and zoning. Chem. Erde-Geochem. 72, 237–244.

Radosavljević, A.S., Stojanović, N.J., Radosavljević-Mihajlović, S.A., Kašić, D.V., 2013. Polymetallic mineralization of the Boranja ore field, Podrinje Metallogenic District, Serbia: zonality, mineral associations and genetic features. Period. Mineral. 82, 61–87.

Radosavljević, A.S., Stojanović, N.J., Radosavljević-Mihajlović, S.A., Vuković, S.N., 2014. Rujevac Sb–Pb–Zn–As polymetallic deposit, Boranja ore field, Western Serbia: native arsenic and arsenic mineralization. Mineral. Petrol. 108, 111–122.

Radosavljević, S., Stojanović, J., Vuković, N., Radosavljević-Mihajlović, A., Kašić, V., 2015. Low-temperature Ni–As–Sb–S mineralization of the Pb(Ag)–Zn deposits within the Rogozna ore field, Serbo-Macedonian Metallogenic Province: ore mineralogy, crystal chemistry and paragenetic relationships. Ore Geol. Rev. 65, 213–227.

Rakić, S., 1962. Classification of genetic types of Pb–Zn deposits related to Tertiary magmatism in the Dinarides on the basis of characteristics mineral assemblages. Proceedings of the Presentations V Counseling, Geological Association of Companies F.N.R. Yugoslavia, part II Mineralogy–Petrology–Ore Deposits, Belgrade, pp. 189–195 (in Serbian and German).

Rakić, S., Đorđević, D., Radosavljević, S., Zarić, P., Dimitrijević, R., Dangić, A., Cvetković, Lj, Kubat, I., 2003. The newly discovered and rare minerals from graizen and pyroclastic rocks of the ore fields of Srebrenica (Bosnia and Herzegovina). 8th Yearbook of Yugoslav Association for Mineralogy, Belgrade, Serbia, pp. 142–150 (in Serbian with English summary).

Ramdohr, P., 1980. The Ore Minerals and Their Intergrowths (Pergamon, Oxford).

Ramović, M., 1963. The zinc–lead–silver veins of Srebrenica (East Bosnia) — Yugoslavia. Geološki Glasnik, Sarajevo, BiH. 1, pp. 1–96 (in Serbian with English summary).

Sack, R.O., Ebel, D.S., 2006. Thermochemistry of sulfide mineral solutions. Rev. Mineral. Geochem. 61, 265–364.

Schneidere, A., 1987. Eruptive processes, mineralization and isotopic evolution of the Los Frailes Karlkari region, Bolivia. Rev. Geol. Chile 3 (30), 27–33.

Seifert, T., Sandmann, D., 2006. Mineralogy and geochemistry of indium-bearing polymetallic vein-type deposits: implications for host minerals from the Freiberg district, Eastern Erzgebirge, Germany. Ore Geol. Rev. 28, 1–31.

Steiger, R.H., Knežević, V., Karamata, S., 1989. Origin of some granitic rocks from the Southern Margin of the Pannonian basin in Western Serbia, Yugoslavia. Terra Abstracts EUG 5 1, pp. 52–53.

Strmic-Palinkas, S., Tasev, G., Serafimovski, T., Palinkas, L., Smajgl, D., Peltekovski, Z., 2013. Ore-fluid evolution at the Sasa Pb–Zn skarn deposit, Republic of Macedonia. AusIMM New Zealand Branch Annual Conference, pp. 487–494.

Thode, H.G., Monster, J., Durford, H.B., 1961. Sulphur isotope geochemistry. Geochim. Cosmochim. Acta 25, 150–174.

Topalović, D., 1984. Vein type of Sb–Pb–Zn ore mineralization of Čumavići (the ore region of Srebrenica). Bulletin of Geoinstitute 17 pp. 77–87 (in Serbian with English summary).

Voudouris, P., Melfos, V., Spry, P.G., Bonsall, T.A., Tarkian, M., Solomos, Ch., 2008. Carbonate-replacement Pb–Zn–Ag ± Au mineralization in the Kamariza area, Lavrion, Greece: Mineralogy and thermochemical conditions of formation. Mineral. Petrol. 94, 85–106.

Vukašinović, S., Stefanović, D., 2003. General characteristics and geological implications of geomagnetic field of the Dinarides and Vardar Zone. Bulletin (Vesnik), Géologie, Hydrogéologie et Géologie D'Ingénier 53, pp. 535–550.

Wagner, T., Cook, N.J., 1998. Sphalerite remobilization during multistage hydrothermal mineralization events — examples from siderite–Pb–Zn–Cu–Sb veins, Rheinisches Schiefergebirge, Germany. Mineral. Petrol. 63, 223–241.

Wang, N., 1978. New data for Ag_8SnS_6 (canfieldite) and Ag_8GeS_6 (argyrodite). Neues Jb. Mineral. Monat. 269–272.

Ye, L., Cook, N.J., Ciobanu, C., Yuping, L., Qian, Z., Tiegeng, L., Wei, G., Yulong, Y., Danyushevski, L., 2011. Trace and minor elements in sphalerite from base metal deposits in South China: A LA–ICPMS. Ore Geol. Rev. 39, 188–217.

Zarić, P., Janković, S., Radosavljević, S., Djordjević, D., 2000. Tin minerals and tin mineralization of the Pb–Zn–Sb–Ag ore deposits of the Srebrenica orefield. Proceedings of International Symposium of Geology and Metallogenic of the Dinarides and the Vardar zone, Banja Luka, BiH, pp. 425–434.

Zebec, V., 1982. Goniometric determination of Srebrenica stibnite. Glasnik Zemaljskog Muzeja, Sarajevo, BiH 21, pp. 53–54 (in Croatian).